

1

2 **Seasonal cycles and trends of water budget components in 18**
3 **river basins across the Tibetan Plateau: a multiple datasets**
4 **perspective**

5

6 Wenbin Liu^a, Fubao Sun^{a,b*}, Yanzhong Li^a, Guoqing Zhang^{c,d}, Yan-Fang Sang^a,

7 Wee Ho Lim^{a,e}, Jiahong Liu^f, Hong Wang^a, Peng Bai^a

8

9 ^aKey Laboratory of Water Cycle and Related Land Surface Processes, Institute of Geographic
10 Sciences and Natural Resources Research, Chinese Academy of Sciences, Beijing 100101, China

11 ^bHexi University, Zhangye 734000, China

12 ^cKey Laboratory of Tibetan Environmental Changes and Land Surface Processes, Institute of
13 Tibetan Plateau Research, Chinese Academy of Sciences, Beijing 100101, China

14 ^dCAS Center for Excellent in Tibetan Plateau Earth Sciences, Beijing 100101, China

15 ^eEnvironmental Change Institute, Oxford University Centre for the Environment, School of
16 Geography and the Environment, University of Oxford, Oxford OX1 3QY, UK

17 ^fKey Laboratory of Simulation and Regulation of Water Cycle in River Basin, China Institute of
18 Water Resources and Hydropower Research, Beijing 100038, China

19

20 **Submitted to:** Hydrology and Earth System Sciences

21 **Corresponding Author:** Dr. Fubao Sun (Sunfb@igsnr.ac.cn), from the Key Laboratory of Water

22 Cycle and Related Land Surface Processes, Institute of Geographic Sciences and Natural

23 Resources Research, Chinese Academy of Sciences (No. A11, Datun Road, Chaoyang District,

24 Beijing 100101, China)

25 **Email Addresses for other authors:** Wenbin Liu (liuwb@igsnr.ac.cn), Yanzhong Li

26 (liy.14b@igsnr.ac.cn), Guoqing Zhang (guoqing.zhang@itpcas.ac.cn), Yan-fang Sang

27 (sangyf@igsnr.ac.cn), Wee Ho Lim (limwh@igsnr.ac.cn), Jiahong Liu (liujh@iwhr.com), Hong

28 Wang (wanghong@igsnr.ac.cn), Peng Bai (baip.11b@igsnr.ac.cn)

29

30

2017/2/15

31 **Highlights**

- 32 ● A water balance approach to quantify monthly evapotranspiration which accounts
33 for the changes in glacier and water storage of Tibetan Plateau
- 34 ● Evaluation of water budget components and trends for 18 river basin in Tibetan
35 Plateau
- 36 ● Discussion of uncertainties arise from multiple datasets used in Tibetan Plateau

37

38 **Abstract.** The dynamics of water budget over the Tibetan Plateau (TP) are not well
39 understood because of the lack of hydroclimatic observations. Based on multi-source
40 datasets over a 30-year period (1982-2011), we investigate the seasonal cycles and
41 trends of water budget components, e.g., precipitation (P), evapotranspiration (ET)
42 and runoff (Q) of 18 river basins in TP. We apply a two-step bias-correction procedure
43 to calculate the basin-scale ET considering the changes in glacier and water storage
44 change. The results indicate that precipitation, which mainly concentrated during
45 June-October (varied among different monsoons impacted basins), is the major
46 contributor to the runoff in the TP basins. The basin-wide snow water equivalent
47 (SWE) was relatively high from mid-autumn to spring for most of the river basins in
48 TP. The water cycle intensified under global warming in most of these basins; receded
49 in the upper Yellow and Yalong sub-river basins due to the weakening East Asian
50 monsoon. Consistent with the warming climate and moistening in the TP and western
51 China, the aridity index (PET/P) in most of the river basins decreased. These results
52 demonstrate the usefulness of integrating the multi-source datasets (e.g., in situ
53 observations, remote sensing products, reanalysis, land surface model simulations and
54 climate model outputs) for hydrological applications in the data-sparse regions. More
55 generally, such approach might offer helpful insights towards understanding the
56 water/energy budgets and sustainability of water resource management practices of
57 data-sparse regions in a changing environment.

58

59 **1 Introduction**

60 As the highest plateau in the globe (the average elevation is higher than 4000 meters

61 above the sea level), the Tibetan Plateau (TP, also called “the roof of the world” or
62 “the third Pole”) is regarded as one of the most vulnerable region under a warming
63 climate and is exposed to strong interactions among atmosphere, hydrosphere,
64 biosphere and cryosphere in the earth system (Duan and Wu, 2006; Yao et al., 2012;
65 Liu et al., 2016b). It serves as the “Asian water tower” from which some major Asian
66 rivers such as Yellow River, Yangtze River, Brahmaputra River, Mekong River, Indus
67 River, etc., originate. It is a vital water resource to support the livelihood of hundreds of
68 millions of people in China and the neighboring Asian countries (Immerzeel et al.,
69 2010; Zhang et al., 2013). Hence sound knowledge of water budget and hydrological
70 regimes of TP and its response to changing environment would have practical
71 relevance for achieving sustainable water resource management and environmental
72 protection in this part of the world (Yang et al., 2014; Chen et al., 2015).

73

74 Despite the importance of TP in this geographic region, advance in hydrological and
75 land surfaces studies in this region has been limited by data scarcity (Zhang et al.,
76 2007; Li F. et al., 2013; Liu X. et al., 2016). For instance, less than 80 observation
77 stations (~10% of a total of ~750 observation station across China) have been
78 established in TP by the Chinese Meteorological Administration (CMA) since the
79 mid-20th century (Wang and Zeng, 2012). These stations are generally sparse and
80 unevenly distributed at relatively low elevation regions, focus only on the
81 meteorological variables and lack of other land surface observations such as
82 evapotranspiration, snow water equivalent and latent heat fluxes. In addition,
83 long-term observations of river discharge, snow depth, lake depth and glacier melts in
84 the TP are also absent (Akhta et al., 2009; Ma et al., 2016). Therefore, the water
85 balance and hydrological regimes for each river basin of TP and their relation with

86 monsoons are poorly understood (Cuo et al., 2014; Xu et al., 2016). Whilst this
87 shortcoming could be resolved through installation of in-situ monitoring systems
88 (Yang et al., 2013; Zhou et al., 2013; Ma et al., 2015), the overall cost of running the
89 operational sites would be substantial. Another workaround would be through
90 modeling approach, i.e., feeding remote sensing information and meteorological
91 forcing data into physically-based land surface model (LSM) to simulate the
92 basin-wide water budget (Bookhagen and Burbank, 2010; Xue et al., 2013; Zhang et
93 al., 2013; Cuo et al., 2015; Zhou et al., 2015; Wang et al., 2016). However, such
94 approach is not immune from the issue of data scarcity at multiple river basins (with
95 varied sizes and/or terrain complexities) for supporting model calibration and
96 validation purposes (Li F. et al., 2014).

97

98 Most recently, several global (or regional) datasets relevant to the calculation of water
99 budget have been released. They include remote sensing-based retrievals (Tapley et al.,
100 2004; Zhang et al., 2010; Long et al., 2014; Zhang Y. et al., 2016), land surface model
101 (LSM) simulations (Rui, 2011), reanalysis outputs (Berrisford et al., 2011; Kobayashi
102 et al., 2015) and gridded forcing data interpolated from the in situ observations
103 (Harris et al., 2014). For example, there are many products related to terrestrial
104 evapotranspiration (ET) such as GLEAM_E (Global Land surface Evaporation: the
105 Amsterdam Methodology, Miralles et al., 2011a), MTE_E (a product integrated the
106 point-wise ET observation at FLUXNET sites with geospatial information extracted
107 from surface meteorological observations and remote sensing in a machine-learning
108 algorithm, Jung et al., 2010), LSM-simulated ETs from Global Land Data
109 Assimilation System version 2 (GLDAS-2) with different land surface schemes
110 (Rodell et al., 2004), ETs from Japanese 55-year reanalysis (JRA55_E), the

111 ERA-Interim global atmospheric reanalysis dataset (ERA-Interim) and the National
112 Aeronautic and Space Administration (NASA) Modern Era Retrospective-analysis
113 for Research and Application (MERRA) reanalysis data (Lucchesi, 2012). Moreover,
114 there are also several global or regional LSM-based runoff simulations from GLDAS
115 and the Variable Infiltration Capacity (VIC) model (Zhang et al., 2014). A few
116 attempts have been made to validate multiple datasets for certain water budget
117 components and to explore their possible hydrological implications. For example, Li
118 X. et al. (2014) and Liu et al. (2016a) evaluated multiple ET estimates against the
119 water balance method at annual and monthly time scales. Bai et al. (2016) assessed
120 streamflow simulations of GLDAS LSMs in five major rivers over the TP based on
121 the discharge observations. Although uncertainties might exist among different
122 datasets with various spatial and temporal resolutions and calculated using different
123 algorithms (Xia et al., 2012), they offer an opportunity to examine the general
124 basin-wide water budgets and their uncertainties in gauge-sparse regions such as the
125 TP considered in this study.

126

127 From the multiple datasets perspective, this study aims to investigate the water budget
128 in 18 TP river basins distributed across the Tibetan Plateau; and evaluate seasonal
129 cycles and annual trends of these water budget components. This paper is organized
130 as follows: the datasets and methods applied in this study are described in Sect.2. The
131 results of season cycles and annual trends of water budget components for the river
132 basins are presented and discussed in Sect.3. The uncertainties arise from employing
133 multiple datasets are also discussed in the same section. In Sect.4, we generalize our
134 findings which would be helpful for understanding the water balances of the river
135 basins under constant influence of interplay between westerlies and monsoons (e.g.,

136 Indian monsoon, East Asian monsoon) in the Tibetan Plateau.

137

138 **2 Data and methods**

139 **2.1 Multiple datasets used**

140 **2.1.1 Runoff, precipitation and terrestrial storage change**

141 We obtained the observed daily runoff (Q) of the study period from the National
142 Hydrology Almanac of China (Table 1). There are < 30% missing data in some
143 gauging stations such as Yajiang, Tongren, Gandatan and Zelingou. Therefore, the
144 VIC Retrospective Land Surface Dataset over China (1952~2012, VIC_IGSNRR
145 simulated) with a spatial resolution of 0.25 degree and a daily temporal resolution
146 from the Geographic Sciences and Natural Resources Research (IGSNRR), Chinese
147 Academy of Sciences, is also used. This dataset is derived from the VIC model forced
148 by the gridded daily observed forcing (IGSNRR_forcing) (Zhang et al., 2014). A
149 degree-day scheme was used in the model to account for the influences of snow and
150 glacier on hydrological processes.

151

152 In terms of precipitation (P), we used the gridded monthly precipitation dataset
153 available at CMA (spatial resolution of 0.5 degree; 1961-2011; interpolated from
154 observations of 2372 national meteorological stations using the Thin Plate Spline
155 method) (Table 1). Since the reliability of this dataset might be restricted by the
156 relatively sparse stations and complex terrain conditions of TP, we make an attempt to
157 incorporate two other precipitation datasets ((IGSNRR_forcing and Tropical Rainfall
158 Measuring Mission TRMM 3B43 V7). The precipitation from IGSNRR forcing
159 datasets (0.25 degree) was derived by interpolating gauged daily precipitation from
160 756 CMA stations based on the synergistic mapping system algorithm (Shepard,

161 1984; Zhang et al., 2014) and was further bias-corrected using the CMA gridded
162 precipitation.

163 <Table 1, here please, thanks>

164 To get the change in terrestrial storage (ΔS), we used of three latest global terrestrial
165 water storage anomaly and water storage change datasets (available on the GRACE
166 Tellus website: <http://grace.jpl.nasa.gov/>) that were retrieved from the Gravity
167 Recovery and Climate Experiment (GRACE, Tapley et al., 2004; Landerer and
168 Swenson, 2012; Long et al., 2014). Briefly, they were processed separately at the Jet
169 Propulsion Laboratory (JPL), the GeoForschungsZentrum (GFZ) and the Center for
170 Space Research at the University of Texas (CSR). To minimize the errors and
171 uncertainty of extracted ΔS , we averaged these GRACE retrievals (2002-2013) from
172 different processing centers in this study.

173

174 **2.1.2 Temperature, potential evaporation and ET**

175 We obtained the monthly gridded temperature dataset (0.5 degree) from CMA; and
176 potential evaporation (PET) dataset (0.5 degree, Harris et al., 2013) from Climatic
177 Research Unit (CRU), University of East Anglia. Moreover, we used six global
178 /regional ET products (four diagnostic products and two LSMs simulations, Table 2),
179 namely (1) GLEAM_E (Miralles et al., 2010, 2011), which consist of three sources of
180 ET (transpiration, soil evaporation and interception) for bare soil, short vegetation and
181 vegetation with a tall canopy calculated using a set of algorithm (www.gleam.eu), (2)
182 GNoah_E simulated using GLDAS-2 with the Catchment Noah scheme
183 (<http://disc.sci.gsfc.nasa.gov/hydrology/data-holdings>) (Rodell et al., 2004), (3)
184 Zhang_E (Zhang et al., 2010), which is estimated using the modified

185 Penman-Monteith equation forced with MODIS data, satellite-based vegetation
186 parameters and meteorological observations (<http://www.ntsug.umt.edu/project/et>), (4)
187 MET_E (Jung et al., 2010) (<https://www.bgc-jena.mpg.de/geodb/projects/Home.phs>),
188 (5) VIC_E (Zhang et al., 2014) from VIC_IGSNRR simulations
189 (http://hydro.igsnr.ac.cn/public/vic_outputs.html) and (6) PML_E (Zhang Y. et al.,
190 2016) computed from global observation-driven Penman-Monteith-Leuning (PML)
191 model (<https://data.csiro.au/dap/landingpage?pid=csiro:17375&v=2&d=true>).

192

193 **2.1.3 Vegetation and snow/glacier parameters**

194 To quantify the dynamics of vegetation of each river basin, we applied the
195 Normalized Difference Vegetation Index (NDVI) and the Leaf Area Index (LAI)
196 (Table 1). Briefly, the NDVI data was obtained from the Global Inventory Modeling
197 and Mapping Studies (GIMMS) (Turker et al., 2005)
198 (https://nex.nasa.gov/nex/projects/1349/wiki/general_data_description_and_access/)
199 while the LAI data was collected from the Global Land Surface Satellite (GLASS)
200 products (<http://www.glcg.umd.edu/data/lai/>) (Liang and Xiao, 2012). Whist the
201 change in seasonal snow cover and glacier has significant impact on the water and
202 energy budgets of TP, it remains a technical challenge to get reliable observations due
203 to harsh environment (especially at the basin scale). However, recently available
204 satellite-based/LSM-simulated products might provide adequate characterization of
205 the variation of snow cover and glacier. To quantify the change in snow cover at each
206 basin, we applied the daily cloud free snow composite product from MODIS
207 Terra-Aqua and the Interactive Multisensor Snow and Ice Mapping System for the
208 Tibetan Plateau (Zhang et al., 2012; Yu et al., 2015), in conjunction with the snow

209 water equivalent (SWE) retrieved from Global Snow Monitoring for Climate
210 Research product (GlobSnow-2, <http://www.globsnow.info/>) and the VIC_IGSNRR
211 simulations (Takala et al., 2011; Zhang et al., 2014). We extracted general distribution
212 of glacier of TP from the Second Glacier Inventory Dataset of China (Guo et al.,
213 2014). All gridded datasets used were first uniformly interpolated to a spatial
214 resolution of 0.5 degree based on the bilinear interpolation to make their
215 inter-comparison possible. The datasets were then extracted for each of TP basins.

216

217 **2.1.4 Monsoon indices**

218 In general, the TP climate is under the influence of the westerlies, Indian summer
219 monsoon and East Asian summer monsoon (Yao et al., 2012). To investigate the
220 changes of monsoon systems and their potential impact on the water budget in the TP
221 basins, we used three monsoon indices, namely Asian Zonal Circulation Index (AZCI),
222 Indian Ocean Dipole Mode Index (IODMI) and East Asian Summer Monsoon Index
223 (EASMI). Briefly, the IODMI is an indicator of the east-west temperature gradient
224 across the tropical Indian Ocean (Saji et al., 1999), which can be downloaded from
225 the following website:

226 <http://www.jamstec.go.jp/frcgc/research/d1/iod/HTML/Dipole%20Mode%20Index.ht>

227 [ml](http://www.jamstec.go.jp/frcgc/research/d1/iod/HTML/Dipole%20Mode%20Index.html). The EASMI and AZCI (60°-150°E) reflect the dynamics of East Asian summer
228 monsoon (Li and Zeng, 2002) and the westerlies (represented by Asian Zonal
229 Circulation index), which can be obtained from Beijing Normal University
230 (<http://ljp.gcess.cn/dct/page/65577>) and the National Climate Center of China
231 (<http://ncc.cma.gov.cn/Website/index.php?ChannelID=43WCHID=5>), respectively.

232

233 **2.1.5 Study basins**

234 In this study, we selected 18 river basins of varied sizes (range: 2832-191235 km² ;
235 see Table 1 for details) with adequate runoff data over a 30-year period (1982-2011).
236 They are distributed in the northwestern, southeastern and eastern parts of the plateau
237 with multiyear-mean and basin-averaged temperature and precipitation ranging from
238 -5.68 to 0.97 °C and 128 to 717 mm, which are solely dominated or under the
239 influences of the westerlies, the Indian Summer monsoon and the East Asian monsoon
240 (Yao et al., 2012). There are more glacier and snow covers in the westerlies-dominant
241 basins such as Yerqiang, Yulongkashi and Keliya (10.86~23.27% and 29.16~35.95%,
242 respectively); less for the East Asian monsoon-dominated basins such as Yellow,
243 Yangtze and Bayin (0~0.96% and 9.42~20.05%, respectively) (Table 2).

244 <Figure 1, here please, thanks>

245 <Table 2, here please, thanks>

246

247 **2.2 Methods**

248 **2.2.1 Water balance-based ET estimation**

249 The basin-wide water balance at the monthly and annual timescales could be written
250 as the principle of mass conservation (also known as the continuity equation, Oliveira
251 et al., 2014) of basin-wide precipitation (P, mm), evapotranspiration (ET_{wb}, mm),
252 runoff (Q, mm) as well as terrestrial water storage change (ΔS , mm),

$$253 \quad ET_{wb} = P - Q - \Delta S \quad (1)$$

254 In most TP basins, glacier melt (M_G, mm) contributes to river discharge together with
255 precipitation (liquid precipitation and snow). The monthly and annual water balance
256 in these basins can thus be revised as,

$$257 \quad ET_{wb} = P + M_G - Q - \Delta S \quad (2)$$

258 Several attempts have been made for separating glacier contributions to river

259 discharge through site-scale isotopic observations, remote sensing as well as
260 land-surface hydrological modeling for some individual TP basins (Zhang et al., 2013;
261 Zhou et al., 2014; Neckel et al., 2014; Xiang et al., 2016). However, accurate
262 quantification of M_G is difficult in the data-sparse TP, especially for multiple basins.
263 In this study, we simply use the percentages of glacier melt to river discharge for
264 some TP basins derived from the literatures (Chen, 1988; Mansur and Ajinisa, 2005;
265 Zhang et al., 2013; Liu J. et al., 2016) and the empirical relations between the glacier
266 area ratio (%) and glacier melt in basins mentioned above (Table 3).

267 <Table 3, here please, thanks>

268 The terrestrial water storage (ΔS) in Eq. (2) includes the surface, subsurface and
269 ground water changes. It has been demonstrated cannot be neglected in water balance
270 calculation over monthly and annual timescales due to snow cover change and
271 anthropogenic interferences (e.g., reservoir operation, agricultural water withdrawal)
272 (Liu et al., 2016a). For the period 2002-2011, we calculated basin-wide ET (ET_{wb})
273 directly using the GRACE-derived ΔS in Eq. (2). Since GRACE data is absent
274 before 2002, we calculated the monthly ET_{wb} using the following two-step
275 bias-correction procedure (Li X. et al., 2014). We defined $P + M_G - Q$ in Eq. (2) as
276 biased ET (ET_{biased} , available from 1982 to 2011) relative to the “true” ET
277 ($ET_{wb} = P + M_G - Q - \Delta S$, available during the period 2002-2011 when the GRACE
278 data is available). Over the period 2002-2011, we first fitted ET_{biased} and ET_{wb}
279 series separately using different gamma distributions, which has been evidenced as an
280 proper method for modeling the probability distribution of ET (Bouraoui et al., 1999).
281 The monthly ET_{biased} series (2002-2011) can then be bias-corrected through the
282 inverse function (F^{-1}) of the gamma cumulative distribution function (CDF, F) of
283 ET_{wb} by matching the cumulative probabilities between two CDFs as follow (Liu et

284 al., 2016a),

$$285 \quad ET_{\text{corrected}}(m) = F^{-1}(F(ET_{\text{biased}}(m)|\alpha_{\text{biased}}, \beta_{\text{biased}})|\alpha_{\text{wb}}, \beta_{\text{wb}}) \quad (3)$$

286 Here $\alpha_{\text{biased}}, \beta_{\text{biased}}$ and $\alpha_{\text{wb}}, \beta_{\text{wb}}$ are shape and scale parameters of
287 gamma distributions for ET_{biased} and ET_{wb} . $ET_{\text{corrected}}(m)$ and $ET_{\text{biased}}(m)$
288 represent the monthly corrected and biased ET, respectively. The bias correction
289 procedure can be flexibly applied to the period 1983-2011 by matching the CDF
290 of ET_{biased} (1983-2011) to that of $ET_{\text{corrected}}$ (2002-2011). The second step of
291 bias correction is to eliminate the annual bias through the ratio of annual
292 ET_{biased} to annual $ET_{\text{corrected}}$ calculated in the first step using the following
293 method,

$$294 \quad ET_{\text{final}}(m) = \frac{ET_{\text{biased}}(a)}{ET_{\text{corrected}}(a)} \times ET_{\text{corrected}}(m) \quad (4)$$

295 where $ET_{\text{final}}(m)$ is the final monthly ET after bias correction. $ET_{\text{biased}}(a)$ and
296 $ET_{\text{corrected}}(a)$ represent the annual biased and corrected ET while
297 $ET_{\text{corrected}}(m)$ is the monthly corrected ET obtained from the first step. The
298 procedure was then applied to correct the monthly ET_{biased} series and
299 calculated the monthly $ET_{\text{corrected}}$ during the period 1982-2001 for all TP
300 basins. We take these results as sufficient representation of the “true” ET (ET_{wb})
301 for evaluating multiple ET products and trend analysis.”

302

303 **2.2.2 Modified Mann-Kendall test method**

304 The Mann-Kendall (MK) test is a rank-based nonparametric approach which is less
305 sensitive to outlier relative to other parametric statistics, but it is sometimes
306 influenced by the serial correlation of time series. Pre-whitening is often used to
307 eliminate the influence of lag-1 autocorrelation before the use of MK test. For

308 example, $X = (X_1, X_2, \dots, X_n)$ is a time series data, it will be replaced by $(X_2 -$
309 $cX_1, X_3 - cX_2, \dots, X_{n+1} - cX_n)$ in pre-whitening if the lag-1 autocorrelation
310 coefficient (c) is larger than 0.1 (von Storch, 1995). However, significant lag- i
311 autocorrelation may still be detected after pre-whitening because only the lag-1
312 autocorrelation is considered in pre-whitening (Zhang et al., 2013). Moreover, it
313 sometimes underestimate the trend for a given time series (Yue et al., 2002). Hamed
314 and Rao (1998) proposed a modified version of MK test (MMK) to consider the lag- i
315 autocorrelation and related robustness of the autocorrelation through the use of
316 equivalent sample size, which has been widely used in previous studies during the last
317 five decades (McVicar et al., 2012; Zhang et al., 2013; Liu and Sun, 2016). In the
318 MMK approach, if the lag- i autocorrelation coefficients are significantly distinct from
319 zero, the original variance of MK statistics will be replaced by the modified one. In
320 this study, we used the MMK approach to quantify the trends of water budget
321 components in 18 TP basins and the significance of trend was tested at the >95%
322 confidence level.

323 **3 Results and Discussion**

324 **3.1 ET evaluation and General hydrological characteristics of 18 TP basins**

325 We first assessed the VIC_IGSNRR simulated runoff against the observations for
326 each basin (for example, at Tangnaihaid and Pangduo stations in Fig.2). If the Nash
327 Efficiency coefficient (NSE) between the observation and simulation is above 0.65,
328 the VIC_IGSNRR simulated runoff is acceptable and could be used to replace the
329 missing values for a given basin. Moreover, the CMA precipitation is consistent with
330 TRMM (Corr = 0.86, RMSE = 8.34 mm/month) and IGSNRR forcing (Corr = 0.94,
331 RMSE = 7.15mm/month) precipitation for multiple basins (and also for the smallest
332 basin above Tongren station, Fig.2), although the observation-derived and

333 TRMM-estimated precipitation also has uncertainties. The magnitudes of
334 GRACE-derived annual mean water storage change (ΔS) in 18 TP basins are
335 relatively less than those for other water balance components such as annual P, Q and
336 ET (Table 4). The uncertainties among GRACE-derived annual mean ΔS from
337 different data processing centers (CSR, GFZ and JPL) are small for 18 basins except
338 for in the basins controlled by Gadatan and Tangnaihahai stations.

339 [< Figure 2, here please, thanks >](#)

340 [< Table 4, here please, thanks >](#)

341 We then evaluated six ET products in 18 TP basins against our calculated ET_{wb} at a
342 monthly basis during the period 1983-2006 (Fig. 3). The ranges of monthly averaged
343 ET among different basins (approximately 4–39 mm month⁻¹) are very close for all
344 products compare to that calculated from the ET_{wb} (6–42 mm month⁻¹). However,
345 GLEAM_E (correlation coefficient: Corr = 0.85 and root-mean-square-error: RMSE =
346 5.69 mm month⁻¹) and VIC_E (Corr = 0.82 and RMSE = 6.16 mm month⁻¹) perform
347 relatively better than others. Although Zhang_E and GNoah_E were found closely
348 correlated to monthly ET_{wb} in the upper Yellow River, the upper Yangtze River,
349 Qiangtang and Qaidam basins (Li X. et al., 2014), they did not exhibit overall good
350 performances (Corr = 0.61, RMSE = 7.97 mm month⁻¹ for Zhang_E and Corr = 0.42,
351 RMSE = 10.16 mm month⁻¹ for GNoah_E) for 18 TP basin used in this study. We thus
352 use GLEAM_E and VIC_E together with ET_{wb} to calculate the seasonal cycles and
353 trends of ET in 18 TP basins in the following sections.

354 [< Figure 3, here please, thanks >](#)

355 To investigate the general hydroclimatic characteristics of rivers over the TP, we
356 classify 18 basins into three categories, namely westerlies-dominated basins
357 (Yerqiang, Yulongkashi and Kelia), Indian monsoon-dominated basins (Brahmaputra

358 and Salween), and East Asian monsoon-dominated basins (Yellow, Yalong and
359 Yangtze) referred to Tian et al. (2007), Yao et al. (2012) and Dong et al. (2016).
360 Interestingly, they are clustered into three groups under Budyko framework (Budyko,
361 1974; Zhang D. et al., 2016) with relatively lower evaporative index in Indian
362 monsoon-dominant basins and higher aridity index in westerlies-dominant basins,
363 which reveal various long-term hydroclimatologic conditions (Fig. 4). Overall, the
364 annual mean air temperature increases (-5.68 ~0.97 °C) while multiyear mean glacier
365 area (and thus the glacier melt normalized by precipitation) decreases (23.27 ~ 0%)
366 gradually from the westerlies-dominant, Indian monsoon-dominant to East Asian
367 monsoon-dominant basins. The vegetation status (NDVI range: 0.05~0.43; LAI range:
368 0.03~0.83) tends to be better and ET increases (and thus runoff coefficient gradually
369 decreases) from cold to warm basins (Fig. 4 and Table 1). The R^2 between
370 basin-averaged NDVI and ET is 0.76 which shows a clear vegetation control on ET in
371 18 TP basins. The results are in line with Shen et al. (2015), which indicated that the
372 spatial pattern of ET trend was significantly and positively correlated with NDVI
373 trend over the TP. The dominant climate systems are overall discrepant for the three
374 TP regions with different water-energy characteristics and sources of water vapor. The
375 westerlies-controlled basins are relatively colder than the Indian monsoon-dominated
376 basins, thus they develop more glaciers (and thus have more snow melt contributions
377 to total river streamflow) and have relatively less vegetation (and thus limit vegetation
378 transpiration). It is a general picture of hydrological regime in high-altitude and cold
379 regions (Zhang et al., 2013; Cuo et al., 2014), which could be interpreted from the
380 perspective of multi-source datasets in the data-sparse TP.

381 < [Figure 4, here please, thanks](#) >

382 **3.2 Seasonal cycles of basin-wide water budget components for the TP basins**

383 The multi-year means of water budget components (i.e., P, Q, ET, snow cover and
384 SWE) and vegetation parameters (i.e., NDVI and LAI) are calculated for each
385 calendar month and for 18 TP river basins using multi-source datasets available from
386 1982 to 2011. Overall, the seasonal variations of P, Q, ET, air temperature and
387 vegetation parameters are similar in all TP basins with peak values occurred in May to
388 September (Fig.5 and Fig.6). The seasonal cycles of snow cover and SWE are
389 generally consistent among the basins (the peak values mainly occur from October to
390 next April, Fig.7). With the ascending air temperature from cold to warm months, the
391 basin-wide precipitation increases and vegetation cover expands gradually (the
392 basin-wide ET also increase). Meanwhile, snow cover and glaciers retreat gradually
393 with the melt water supplying the river discharge together with precipitation. The
394 inter-basin variations of hydrological regime are to a large extent linked to the climate
395 systems that prevail over the TP.

396 [< Figure 5, here please, thanks >](#)

397 Although the temporal patterns of hydrological components are generally analogous,
398 they vary among the parameters, climate zones and even basins (Zhou et al., 2005).
399 For example, relative to air temperature, the seasonal pattern of runoff is similar to
400 precipitation which reveals that runoff is mainly controlled by precipitation in most
401 TP basins. It is in agreement with that summarized by Cuo et al. (2014). In the
402 westerlies-dominated basins, the peak values of precipitation and runoff mainly
403 concentrate in June-August, which contribute approximately 68-82% and 67-78% of
404 annual totals, respectively. During this period, the runoff always exceeds precipitation
405 which indicates large contributions of glacier/snow-melt water to streamflow. It is
406 consistent with the existing findings in Tarim River (Yerqiang, Yulongkashi and
407 Keliya rivers are the major tributaries of Tarim River), which indicated that the melt

408 water accounted for about half of the annual total streamflow (Fu et al., 2008). The
409 ET (vegetation cover) in three westerlies-dominated basins are relatively less (scarcer)
410 than that in other TP basins while the percentages of glacier and seasonal snow cover
411 are higher in these basins which contribute more melt water to river discharge (Fig.6
412 and Fig.7). Overall, the SWE in Yerqiang, Yulongkashi and Keliya rivers are higher in
413 winter than other seasons, but they vary with basins and products which reflect
414 considerable uncertainties in SWE estimations.

415 [< Figure 6, here please, thanks >](#)

416 In the Indian monsoon and East Asian monsoon-dominated basins, the runoff
417 concentrates during June-September (or June- October) with precipitation being the
418 dominant contributor of annual total runoff. For example, the peak values of
419 precipitation and runoff occur during June-September at Zhimenda station
420 (contributing about 80% and 74% of the annual totals) while those occur during
421 June-October at Tangnaihai station (contributing about 78% and 71% of the annual
422 totals, respectively). The results are quite similar to the related studies in eastern and
423 southern TP such as Liu (1999), Dong et al. (2007), Zhu et al. (2011), Zhang et al.
424 (2013), Cuo et al. (2014). The vegetation cover (ET) in most basins is denser (higher)
425 than that in the westerlies-dominant basins. Moreover, the seasonal snow mainly
426 covers from mid-autumn to spring and correspondingly the SWE is relatively higher
427 in these months in all basins except for Yellow River above Xining station, Salwee
428 River above Jiayuqiao station and Brahmaputra River above Nuxia and Yangcun
429 stations.

430 [< Figure 7, here please, thanks >](#)

431 **3.3 Trends of basin-wide water budget components for the TP basins**

432 The hydrological cycle has intensified in the westerlies-dominated basins with Q, P

433 and ET_{wb} all ascended under regional warming (Fig.8), especially in the Keliya
434 River basin (Numaitilangan station). The aridity index (PET/P), which is an indicator
435 for the degree of dryness, slightly declined in all basins in northwestern TP. Although
436 both P and PET were found increase since the 1980s (Shi et al., 2003; Yao et al.,
437 2014), the declined PET/P is, to some extent, attributed to the ascending P exceed the
438 increase in PET in these basins (except for the Yulongkashi basin). The climate
439 moistening (Shi et al., 2003) in the headwaters of these inland rivers would be
440 beneficial to the water resources and oasis agro-ecosystems in the middle and lower
441 basins. The increase in streamflow was also found in most tributaries of the Tarim
442 River (Sun et al., 2006; Fu et al., 2010; Mamat et al., 2010).

443

444 Moreover, the westerlies, revealed by the Asian Zonal Circulation Index (60° - 150° E),
445 slightly enhanced (linear trend: 0.21) over the period 1982-2011 (Fig.9). With the
446 strengthening westerlies, more water vapor may be transported and fell as
447 precipitation or snow in northwestern TP (e.g., the eastern Pamir region). Both SWE
448 products (VIC_IGSNRR simulated and GlobaSnow-2 product) showed slight increase
449 across all basins with rising seasonal snow covers and glaciers (Yao et al., 2012).
450 More precipitation was transformed into snow or glacier and the runoff coefficient
451 (Q/P) exhibited decrease although precipitation obviously increased (Fig.8). In
452 addition, the transpiration in these basins might decrease with vegetation degradation
453 as revealed by the NDVI and LAI (Yin et al., 2016) but the atmospheric evaporative
454 demand indicated by CRU PET increased (significantly increase in the Yulongkashi
455 and Keliya rivers) during the period 1982-2011.

456 < [Figure 8, here please, thanks](#)>

457 < [Figure 9, here please, thanks](#)>

458 In the East Asian monsoon-dominated basins, there are two types of change for
459 basin-wide water budget components. For example, P and Q slightly decreased in the
460 upper Yellow River (Tangnihai, Huangheyuan and Jimai stations) and Yalong River
461 (Yajiang station) but increased in other basins (Zelingou, Gandatan, Xining, Tongren
462 and Zhimenda stations) over the period of 1982-2011 (Fig.10). The decline in Q and P
463 for the upper Yellow and Yalong Rivers (locate at the eastern Tibetan Plateau) were
464 consistent with that found by Cuo et al. (2013, 2014) as well as Yang et al. (2014), and
465 were in line with the weakening (linear slope: -0.01) of the East Asian Summer
466 Monsoon (Fig.9). The vegetation turned green while ET_{wb} and PET increased in all
467 nine basins with the significantly ascending air temperature during the period
468 1982-2011. The aridity index (PET/P) decreased in all basins except for the upper
469 Yellow River basin above Jimai station and the upper Yalong River basin above
470 Yajiang station. Moreover, both the runoff coefficients and SWE decreased except for
471 the Bayin River above Zelingou station and the upper Yellow River above Tongren
472 station in the East Asian monsoon dominated basins.

473 < Figure 10, here please, thanks >

474 The hydrological cycle intensified in the Indian monsoon-dominated basins such as
475 Salween River and Brahmaputra River (Fig.11), in line with the strengthening (linear
476 trend: 0.01) of the Indian summer monsoon (revealed by the Indian Ocean Dipole
477 Mode Index) during the specific period 1982-2011 (Fig.9). In the six basins, trends in
478 P, Q and ET_{wb} are all upward. For example, at Jiayuqiao station, the annual
479 streamflow showed slightly increasing trend which was consistent with that examined
480 during 1980-2000 by Yao et al. (2012). The vegetation status, revealed by NDVI and
481 LAI, turned better with the ascending air temperature. The aridity index (PET/P)
482 decreased in all basins except for the Brahmaputra River above Tangjia station, which

483 indicated that most basins in the Indian monsoon-dominated regions turn wet over the
484 period of 1982-2011. The runoff coefficient (Q/P) increased at Gongbujiangda and
485 Nuxia while decreased at Jiayuqiao, Pangduo, Tangji and Yangcun stations. Moreover,
486 the basin-wide SWE declined in the upper Salween River and Brahmaputra River
487 above Pangduo, Tangjia and Gongbujiangda stations while increased in Brahmaputra
488 River above Nuxia and Yangcun stations.

489 [< Figure 11, here please, thanks >](#)

490 **3.4 Uncertainties**

491 The results may unavoidably associate with several aspects of uncertainties inherited
492 from the multi-source datasets. For example, although the seasonal cycles of ET_{wb}
493 can be captured by GLEAM_E and VIC_E, they still have considerable uncertainties
494 at some stations (e.g., Numaitilangan, Gongbujiangda and Nuxia) (Fig.5). Compared
495 to the annual trend of ET_{wb} (Table 4), most ET products (including the
496 well-performed GLEAM_E and VIC_E in some basins) cannot detect the decreasing
497 trends in 7 out of 18 basins (at Kulukelangan, Tongguziluoke, Xining, Tongren, Jimai,
498 Nuxia and Gongbujiangda stations) due to their different forcing data; algorithm used
499 as well as varied spatial-temporal resolutions (Xue et al., 2013; Li et al., 2014; Liu et
500 al., 2016a). In particular, it is well known that land surface models have some
501 difficulties (e.g., parameter tuning in boundary layer schemes) when applying to the
502 TP, even though they have good performances in different regimes (Xia et al., 2012;
503 Bai et al., 2016). For example, Xue et al. (2013) indicated that GNoah_E
504 underestimated the ET_{wb} in the upper Yellow River and Yangtze River basins on the
505 Tibetan Plateau mainly due to its negative-biased precipitation forcing. We thus only
506 used ET_{wb} in the trend detection of water budget components in Fig.8, Fig.10 and
507 Fig.11 in this study. The two SWE products also showed large uncertainty with

508 respect to both their seasonal cycles and trends. The VIC_IGSNRR simulated and
509 GlobaSnow-2 SWEs have not been validated in the TP due to the lack of snow water
510 equivalent observations, but in some basins (e.g., Zelingou and Numaitilangan) they
511 showed similar seasonal cycles and annual trends.

512

513 Moreover, the interpolation of missing values of runoff with VIC_IGSNRR simulated
514 runoff and the gridded precipitation data (which interpolated from limited gauged
515 precipitation over the plateau) also introduced uncertainties. There are also
516 considerable uncertainties arising from empirical extending the ET series back prior
517 to the GRACE era. Finally, we obtained the contributions of glacier-melt to discharge
518 in some basins from the literatures and took them as constant numbers. It may inherit
519 considerable uncertainty from varied studies using different approaches such as
520 glacier mass-balance observation, isotope observation and hydrological modeling, and
521 the contribution rates would also change under a warming climate. However, reliable
522 quantification of the contribution of glacier-melt to discharge is technically
523 challenging, especially for the data-sparse basins. With these caveats, we can interpret
524 the general hydrological regimes and their responses to the changing climate in the TP
525 basins from solely the perspective of multi-source datasets, which are comparable to
526 the existing studies based on the in situ observations and complex hydrological
527 modeling.

528 [<Table 5, here please, thanks>](#)

529 **4 Summary**

530 In this study, we investigated the seasonal cycles and trends of water budget
531 components in 18 TP basins during the period 1982-2011, which is not well
532 understood so far due to the lack of adequate observations in the harsh environment,

533 through integrating the multi-source global/regional datasets such as gauge data,
534 satellite remote sensing and land surface model simulations. By using a two-step bias
535 correction procedure, we calculated the annual basin-wide ET_{wb} through the water
536 balance approach considering the impacts of glacier and water storage change. We
537 found that the GLEAM_E and VIC_E perform better relative to other products against
538 the calculated ET_{wb} .

539

540 From the Budyko framework perspective, the general water and energy budgets are
541 different in the westerlies-dominated (with higher aridity index, runoff coefficient and
542 glacier cover), the Indian monsoon-dominated and the East Asian
543 monsoon-dominated (with higher air temperature, vegetation cover and
544 evapotranspiration) basins. In the 18 TP basins, precipitation is the major contributor
545 to the river runoff, which concentrates mainly during June-October (June-August for
546 the westerlies-dominated basins, June-September or June to October for the Indian
547 monsoon-dominated and the East Asian monsoon-dominated basins). The basin-wide
548 SWE is relatively high from mid-autumn to spring for all 18 TP basins except for
549 Keliya River and Brahmaputra River above the Nuxia and Yangcun stations. The
550 vegetation cover is relatively less whereas snow/glacier cover is more in the
551 westerlies-dominant basins compared to other basins. In the period 1982-2011, we
552 found that hydrologic cycle intensified across most of the basins in Tibetan Plateau;
553 receded at some tributaries located at the upper Yellow River and Yalong River (due
554 to weakening East Asian monsoon). The aridity index (PET/P) exhibited decrease in
555 most TP basins which corresponded to the warming and moistening climate in the TP
556 and western China. Moreover, the runoff coefficient (Q/P) declined in most basins
557 which may be, to some extent, due to ET increase induced by vegetation greening and

558 the influences of snow and glacier changes. Although there are considerable
559 uncertainties inherited from multi-source data used, the general hydrological regimes
560 in the TP basins could be revealed, which are consistent to the existing results
561 obtained from in situ observations and complex land surface modeling. It indicated
562 the usefulness of integrating the multiple datasets (e.g., in situ observations, remote
563 sensing-based products, reanalysis outputs, land surface model simulations and
564 climate model outputs) for hydrological applications. The generalization here could
565 be helpful for understanding the hydrological cycle and supporting sustainable water
566 resources management and eco-environment protection in the Tibetan Plateau under
567 global warming.

568

569 ***Author contributions.*** Wenbin Liu and Fubao Sun developed the idea to see the
570 general water budgets in the TP basins from the perspective of multisource datasets.
571 Wenbin Liu collected and processed the multiple datasets with the help of Yanzhong
572 Li, Guoqing Zhang, Wee Ho Lim, Hong Wang as well as Peng Bai, and prepared the
573 manuscript. The results were extensively commented and discussed by Fubao Sun,
574 Jiahong Liu and Yan-Fang Sang.

575

576 ***Acknowledgements.*** This study was supported by the National Key Research and
577 Development Program of China (2016YFC0401401 and 2016YFA0602402), National
578 Natural Science Foundation of China (41401037 and 41330529), the Open Research
579 Fund of State Key Laboratory of Desert and Oasis Ecology in Xinjiang Institute of
580 Ecology and Geography, Chinese Academy of Sciences (CAS), the CAS Pioneer
581 Hundred Talents Program (Fubao Sun), the CAS President's International Fellowship
582 Initiative (2017PC0068) and the program for the "Bingwei" Excellent Talents from
583 the Institute of Geographic Sciences and Natural Resources Research, CAS. We are

584 grateful to the NASA MEaSUREs Program (Sean Swenson) for providing the
585 GRACE land data processing algorithm. The basin-wide water budget series in the TP
586 Rivers used in this study are available from the authors upon request
587 (liuwb@igsnrr.ac.cn). We thank the editors and reviewers for their invaluable
588 comments and constructive suggestions.

589

590 **References**

- 591 Akhtar, M., Ahmad, N., and Booij, M.J.: Use of regional climate model simulations as input for
592 hydrological models for the Hindukush-Karakorum-Himalaya region, *Hydrol. Earth Syst. Sci.*
593 13, 1075-1089, 2009.
- 594 Bai, P., Liu, X.M., Yang, T.T., Liang, K., and Liu, C.M.: Evaluation of streamflow simulation
595 results of land surface models in GLDAS on the Tibetan Plateau, *J. Geophys. Res. Atmos.*, 121,
596 12180-12197, 2016.
- 597 Berrisford, P, Lee, D., Poli, P., Brugge, R., Fielding, K., Fuentes, M., Kallberg, P., Kobayashi, S.,
598 Uppala, S., and Simmons, A.: The ERA-interim archive. ERA Reports Series No. 1 Version 2.0,
599 Available from: <[https://www.researchgate.net/publication/41571692_The_ERA-interim](https://www.researchgate.net/publication/41571692_The_ERA-interim_archive)
600 archive>, 2011.
- 601 Bookhagen, B. and Burbank, D.W.: Toward a complete Himalayan hydrological budget:
602 spatiotemporal distribution of snowmelt and rainfall and their impact on river discharge, *J.*
603 *Geophys. Res.*, 115, F03019, 2010.
- 604 Bouraoui, F., Vachaud, G., Li, L.Z.X., LeTreut, H., and Chen, T.: Evaluation of the impact of
605 climate changes on water storage and groundwater recharge at the watershed scale, *Clim. Dyn.*,
606 15(2), 153-161, 1999.
- 607 Budyko, M.I.: *Climate and life*. Academic Press, 1974.
- 608 Chen, D., Xu, B., Yao, T., Guo, Z., Cui, P., Chen, F., Zhang, R., Zhang, X., Zhang, Y., Fan, J., Hou,
609 Z., and Zhang, T.: Assessment of past, present and future environmental changes on the Tibetan
610 Plateau, *Chinese SCI. Bull.*, 60(32), 3025-3035, 2015 (in Chinese).
- 611 Chen, J.: Lichenometrical studies on glacier changes during the Holocene Epoch at the sources

612 region of Urumqi River, *Sci. China B.*, 18(1), 95-104, 1988 (in Chinese).

613 Cuo, L., Zhang, Y.X., Bohn, T.J., Zhao, L., Li, J.L., Liu, Q.M., and Zhou, B.R.: Frozen soil
614 degradation and its effects on surface hydrology in the northern Tibetan Plateau, *J. Geophys.*
615 *Res. Atmos.*, 120(6), 8276-8298, 2015.

616 Cuo, L., Zhang, Y.X., Gao, Y., Hao, Z., and Cairang, L.: The impacts of climate change and land
617 cover/use transition on the hydrology in the upper Yellow River Basin, China, *J. Hydrol.*, 502,
618 37-52, 2013.

619 Cuo, L., Zhang, Y.X., Zhu, F.X., and Liang, L.Q.: Characteristics and changes of streamflow on
620 the Tibetan Plateau: A review, *J. Hydrol. Reg. stud.*, 2, 49-68, 2014.

621 Dong, X., Yao, Z., and Chen, C.: Runoff variation and responses to precipitation in the source
622 regions of the Yellow River, *Resour. Sci.*, 29(3), 67-73, 2007 (in Chinese).

623 Dong, W., Lin, Y., Wright, J.S., Ming, Y., Xie, Y., Wang, B., Luo, Y., Huang, W., Huang, J., Wang,
624 L., Tian, L., Peng, Y., and Xu, F.: Summer rainfall over the southwestern Tibetan Plateau
625 controlled by deep convection over the Indian Subcontinent, *Nat. Commun.*, 7, 10925, 2016.

626 Duan, A.M. and Wu, G.X.: Change of cloud amount and the climate warming on the Tibetan
627 Plateau, *Geophys. Res. Lett.*, 33, L22704, 2006.

628 Fu, L., Chen, Y., Li, W., Xu, C., and He, B.: Influence of climate change on runoff and water
629 resources in the headwaters of the Tarim River, *Arid Land Geogr.*, 31(2), 237-242, 2008 (in
630 Chinese).

631 Fu, L., Chen, Y., Li, W., He, B., and Xu, C.: Relation between climate change and runoff volume
632 in the headwaters of the Tarim River during the last 50 years., *J. Desert Res.*, 30(1), 204-209,
633 2010 (in Chinese).

634 Guo, W.Q., Liu, S.Y., Yao, X.J., Xu, J.L., Shangguan, D.H., Wu, L.Z., Zhao, J.D., Liu, Q., Jiang,
635 Z.L., Wei, J.F., Bao, E.J., Yu, P.C., Ding, L.F., Li, G., Ge, C.M., and Wang, Y.: The Second
636 Glacier Inventory Dataset of China, Cold and Arid Regions Science Data Center at Lanzhou,
637 doi: 10.3972/glacier.001.2013.db, 2014.

638 Hamed, K.H. and Rao, A.R.: A modified Mann-Kendall trend test for autocorrelation data,
639 *J. Hydrol.*, 204(1-4), 182-196, 1998.

640 Huffman, G.J., , E.F., Bolvin, D.T., Nelkin, E.J., and Adler, R.F.: last updated 2013: TRMM

641 Version 7 3B42 and 3B43 Data Sets, NASA/GSFC, Greenbelt, MD. Data set accessed at
642 [http://mirador.gsfc.nasa.gov/cgi-bin/mirador/](http://mirador.gsfc.nasa.gov/cgi-bin/mirador/presentNavigation.pl?tree=project&project=TRMM&dataGroup=Gridded&CGIS)
643 [presentNavigation.pl?tree=project&project=TRMM&dataGroup=Gridded&CGIS](http://mirador.gsfc.nasa.gov/cgi-bin/mirador/presentNavigation.pl?tree=project&project=TRMM&dataGroup=Gridded&CGIS)
644 [ESSID=5d12e2ffa38ca2aac6262202a79d882a](http://mirador.gsfc.nasa.gov/cgi-bin/mirador/presentNavigation.pl?tree=project&project=TRMM&dataGroup=Gridded&CGIS), 2012.

645 Harris, I., Jones, P.D., Osborn, T.J., and Lister, D.H.: Updated high-resolution grids of monthly
646 climatic observations – the CRU TS3.10 Dataset, *Int. J. Climatol.*, 34 (3), 623-642, 2014.

647 Immerzeel, W.W., van Beek, L.P.H., and Bierkens, M.F.P.: Climate change will affect the Asian
648 water towers, *Science*, 328, 1382-1385, 2010.

649 Jung, M., Reichstein, M., Ciais, P., Seneviratne, S.I., Sheffield, J., Goulden, M.L., Bonan, G.,
650 Cescatti, A., Chen, J., de Jeu, R., Dolman, A.J., Eugster, W., Gerten, D., Gianelle, D., Gobron, N.,
651 Heinke, J., Kimball, J., Law, B.E., Montagnani, L., Mu, Q., Mueller, B., Oleson, K., Papale, D.,
652 Richardson, A.D., Rouspard, O., Running, S., Tomelleri, E., Viovy, N., Weber, U., Williams, C.,
653 Wood, E., Zaehle, S., and Zhang, K.: Recent decline in the global land evapotranspiration trend
654 due to limited moisture supply, *Nature*, 467, 951-954, 2010.

655 Kobayashi, S., Ota, Y., Harada, Y., Ebata, A., Moriya, M., Onoda, H., Onogi, K., kamahori, H.,
656 kobayashi, C., Endo, H., miyaoka, K., and Takahashi, K.: The JRA-55 Reanalysis: General
657 specifications and basic characteristics, *J.Meteor. Soc. Japan*, 93(1), 5-58, doi:
658 10.2151/jmsj.2015-001, 2015.

659 Landerer, F.W. and Swenson, S.C.: Accuracy of scaled GRACE terrestrial water storage estimates,
660 *Water Resour.Res.*, 48, W04531, 2012.

661 Li, F.P., Zhang, Y.Q., Xu, Z.X., Liu, C.M., Zhou, Y.C., and Liu, W.F.: Runoff predictions in
662 ungauged catchments in southeast Tibetan Plateau, *J. Hydrol.*, 511, 28-38, 2014.

663 Li, F.P., Zhang, Y.Q., Xu, Z.X., Teng, J., Liu, C.M., Liu, W.F., and Mpelasoka, F.: The impact of
664 climate change on runoff in the southeastern Tibetan Plateau, *J. Hydrol.*, 505, 188-201, 2013.

665 Li, J.P. and Zeng, Q.C.: A unified monsoon index, *Geophys. Res. Lett.*, 29(8), 1274, 2002.

666 Li, X.P., Wang, L., Chen, D.L., Yang, K., and Wang, A.H.: Seasonal evapotranspiration changes
667 (1983-2006) of four large basins on the Tibetan Plateau, *J. Geophys. Res.*, 119 (23),
668 13079-13095, 2014.

669 Liang, S.L. and Xiao, Z.Q.: Global Land Surface Products: Leaf Area Index Product Data
670 Collection(1985-2010), Beijing Normal University, doi:10.6050/glass863.3004.db, 2012.

671 Liu, J., Liu, T., Bao, A., De Maeyer, P., Feng, X., Miller, S.N., and Chen, X.: Assessment of
672 different modeling studies on the spatial hydrological processes in an arid alpine catchment,
673 *Water Resour. Manag.*, 30, 1757-1770, 2016.

674 Liu, T.: Hydrological characteristics of Yalungzangbo River, *Acta Geogr. Sin.*, 54 (Suppl.),
675 157-164, 1999 (in Chinese).

676 Liu, W.B. and Sun, F.B.: Assessing estimates of evaporative demand in climate models using
677 observed pan evaporation over China, *J. Geophys. Res. Atmos.*, 121, 8329-8349, 2016.

678 Liu, W.B., Wang, L., Zhou, J., Li, Y.Z., Sun, F.B., Fu, G.B., Li, X.P., and Sang, Y-F.: A worldwide
679 evaluation of basin-scale evapotranspiration estimates against the water balance method, *J.*
680 *Hydrol.*, 538, 82-95, 2016a.

681 Liu, W.B., Wang, L., Chen, D.L., Tu, K., Ruan, C.Q., and Hu, Z.Y.: Large-scale circulation
682 classification and its links to observed precipitation in the eastern and central Tibetan Plateau,
683 *Clim. Dyn.*, 46, 3481-3497, 2016b.

684 Liu, X.M., Yang, T., Hsu, K., Liu, C., and Sorooshian, S.: Evaluating the streamflow simulation
685 capability of PERSIANN-CDR daily rainfall products in two river basins on the Tibetan Plateau,
686 *Hydrol. Earth Syst. Sci. Discuss.*, doi: 10.5194/hess-20160282, 2016.

687 Long, D., Shen, Y.J., Sun, A., Hong, Y., Longuevergne, L., Yang, Y.T., Li, B., and Chen, L.:
688 Drought and flood monitoring for a large karst plateau in Southwest China using extended
689 GRACE data, *Remote Sen. Environ.*, 155, 145-160, 2014.

690 Lucchesi, R.: File specification for MERRA products, GMAO Office Note No.1 (version 2.3), 82
691 pp, available from http://gmao.gsfc.nasa.gov/pubs/office_notes, 2012.

692 Ma, N., Szilagyi, J., Niu, G.Y., Zhang, Y.S., Zhang, T., Wang, B.B., and Wu, Y.H.: Evaporation
693 variability of Nam Co Lake in the Tibetan Plateau and its role in recent rapid lake expansion, *J.*
694 *Hydrol.*, 537, 27-35, 2016.

695 Ma, N., Zhang, Y.S., Guo, Y.H., Gao, H.F., Zhang, H.B., and Wang, Y.F.: Environmental and
28 / 55

696 biophysical controls on the evapotranspiration over the highest alpine steppe, *J. Hydrol.*, 529,
697 980-992, 2015.

698 Mamat, A., Halik, W., and Yang, X.: The climatic changes of Qarqan river basin and its impact on
699 the runoff, *Xinjiang Agric. Sci.*, 47 (5), 996-1001, 2010 (in Chinese).

700 Mansur, S. and Ajinisa, T.: An analysis of water resources and it's hydrological characteristics of
701 Yarkend River Valley, *J. Xinjiang Norm. Univ. (Nat. Sci. Ed.)*, 24(1), 74-78, 2005 (in Chinese).

702 McVicar, T.R., Roderick, M., Donohue, R.J., Li, L.T., Van Niel, T.G., Thomas, A., Grieser, J.,
703 Jhajharia, D., Himri, Y., Mahowald, N.M., Mescherskaya, A.V., Kruger, A.C., Rehman, S., and
704 Dinpashoh, Y.: Global review and synthesis of trends in observed terrestrial near-surface wind
705 speeds: implications for evaporation, *J. Hydrol.*, 416-417, 182-205, 2012.

706 Miralles, D.G., De Jeu, R.A.M., Gash, J.H., Holmes, T.R.H., and Dolman, A.J.: Magnitude and
707 variability of land evaporation and its components at the global scale, *Hydrol. Earth Syst. Sci.*, 15,
708 967-981, 2011.

709 Miralles, D.G., Gash, J.H., Holmes, T.R.H., de Jeu, R.A.M, and Dolman, A.J.: Global canopy
710 interception from satellite observations, *J. Geophys. Res.*, 115, D16122, 2010.

711 Neckel, N., Kropáček, J., Bolch, T., and Hochschild, V.: Glacier mass changes on the Tibetan
712 Plateau 2003-2009 derived from ICESat laser altimetry measurements, *Environ. Res. Lett.*, 9,
713 014009(7pp), 2014.

714 Oliveira, P.T.S., Mearing, M.A., Moran, M.S., Goodrich, D.C., Wendland, E., and Gupta, H.V.:
715 Trends in water balance components across the Brazilian Cerrado, *Water Resour. Res.*, 50,
716 7100-7114, 2014.

717 Rodell, M., Houser, P.R., Jambor, U., Gottschalck, J., Mitchell, K., Meng, C.-J., Arsenault, K.,
718 Cosgrove, B., Radakovich, J., Bosilovich, M., Entin, J.K., Walker, P., Lohmann, D., and Toll, D.:
719 The global land data assimilation system, *B. Am. Meteorol. Soc.*, 85, 381-394, 2004.

720 Rui, H.: README Document for Global Land Data Assimilation System Version 2 (GLDAS-2)
721 Products, GES DISC, 2011.

722 Saji, N.H., Goswami, B.N., Vinayachandran, P.N., and Yamagata, T.: A dipole mode in the tropical
723 Indian Ocean, *Nature*, 401, 360-363, 1999.

724 Shen, M.G., Piao, S.L., Jeong, S., Zhou, L.M., Zeng, Z.Z., Ciais, P., Chen, D.L., Huang, M.T., Jin,
725 C.S., Li, L.Z.X., Li, Y., Myneni, R.B., Yang, K., Zhang, G.X., Zhang, Y.J., and Yao, T.D.:
29 / 55

726 Evaporative cooling over the Tibetan Plateau induced by vegetation growth, *Proc. Natl. Acad.*
727 *Sci. U. S.A.*, 112(30), 9299-9304, 2015.

728 Shi, Y.F., Shen, Y.P., Li, D.L., Zhang, G.W., Ding, Y.J., Hu, R.J., and Kang, E.S.: Discussion on
729 the present climate change from Warm2dry to Warm2wet in northwest China, *Quat. Sci.*, 23(2),
730 152-164, 2003 (in Chinese).

731 Shepard, D.S.: Computer mapping: the SYMAP interpolation algorithm. *Spatial Statistics and*
732 *Models*, G.L. Gaile and C.J. Willmott, Eds., D. Reidel, 133-145, 1984.

733 Sun, B., Mao, W., Feng, Y., Chang, T., Zhang, L., and Zhao, L.: Study on the change of air
734 temperature, precipitation and runoff volume in the Yarkant River basin, *Arid Zone Res.*, 23(2),
735 203-209, 2006 (in Chinese).

736 Takala, M., Luojus, K., Pulliainen, J., Derksen, C., Lemmetyinen, J., Kärnä J.-P., Koskinen, J., and
737 Bojkov, B.: Estimating northern hemisphere snow water equivalent for climate research through
738 assimilation of spaceborne radiometer data and ground-based measurements, *Remote*
739 *Sens. Environ.*, 115 (12), 3517-3529, 2011.

740 Tapley, B.D., Bettadpur, S., Watkins, M., and Reigber, C.: The gravity recovery and climate
741 experiment: mission overview and early results, *Geophys. Res. Lett.*, 31, L09607, 2004.

742 Tian, L., Yao, T., MacClune, K., White, J.W.C., Schilla, A., Vaughn, B., Vachon, R., and
743 Ichiyanagi, K.: Stable isotopic variations in west China: a consideration of moisture sources, *J.*
744 *Geophys. Res. Atmos.*, 112, D10112, 2007.

745 Tucker, C.J., Pinzon, J.E., Brown, M.E., Slayback, D., Pak, E.W., Mahoney, R., Vermote, E., and
746 El Saleous, N.: An extended AVHRR 8 km NDVI data set compatible with MODIS and SPOT
747 vegetation NDVI data, *Int. J. Remote Sens.*, 26(20), 4485-4498, 2005.

748 von Storch, H.: Misuses of statistical analysis in climate research, In *Analysis of Climate*
749 *Variability: Applications of Statistical Techniques*, Springer-Verlag: Berlin, 11-26, 1995.

750 Wang, A. and Zeng, X.: Evaluation of multireanalysis products within site observations over the
751 Tibetan Plateau, *J. Geophys. Res.*, 117, D05102, 2012.

752 Wang, L., Sun, L.T., Shrestha, M., Li, X.P., Liu, W.B., Zhou, J., Yang, K., Lu, H., and Chen, D.L.:
753 Improving snow process modeling with satellite-based estimation of

754 near-surface-air-temperature lapse rate, *J. Geophys. Res. Atmos.*, 121, 12005-12030, 2016.

755 Xia, Y., Mitchell, K., Ek, M., Cosgrove, B., Sheffield, J., Luo, L., Alonge, C., Wei, H., Meng, J.,
756 Livneh, B., and Duang, Q.: Continental-scale water and energy flux analysis and validation for
757 North American Land Data Assimilation System project phase 2 (NLDAS-2): 2. Validation of
758 model-simulated streamflow, *J. Geophys. Res. Atmos.*, 117(D3), D03110, 2012.

759 Xiang, L., Wang, H., Steffen, H., Wu, P., Jia, L., Jiang, L., and Shen, Q.: Groundwater storage
760 changes in the Tibetan Plateau and adjacent areas revealed from GRACE satellite gravity data,
761 *Earth Planet. Sci. Lett.*, 449, 228-239, 2016.

762 Xu, L.: The land surface water and energy budgets over the Tibetan Plateau, Available from
763 Nature Precedings < <http://hdl.handle.net/10101/npre.2011.5587.1>>, 2011.

764 Xue, B.L., Wang, L., Yang, K., Tian, L., Qin, J., Chen, Y., Zhao, L., Ma, Y., Koike, T., Hu, Z., and
765 Li, X.P.: Modeling the land surface water and energy cycle of a mesoscale watershed in the
766 central Tibetan Plateau with a distributed hydrological model, *J. Geophys. Res. Atmos.*, 118,
767 8857-8868, 2013.

768 Yao, Z., Duan, R., and Liu, Z.: Changes in precipitation and air temperature and its impacts on
769 runoff in the Nujiang River basins. *Resour. Sci.* 34(2), 202-210, 2012 (in Chinese)

770 Yang, K., Qin, J., Zhao, L., Chen, Y.Y., Tang, W.J., Han, M.L., Lazhu, Chen, Z.Q., Lv, N., Ding,
771 B.H., Wu, H., and Lin, C.G.: A multi-scale soil moisture and freeze-thaw monitoring network
772 on the third pole, *Bull. Am. Meteorol. Soc.*, 94,1907-1916, 2013.

773 Yang, K., Wu, H., Qin, J., Lin, C.G., Tang, W.J., and Chen, Y.Y.: Recent climate changes over the
774 Tibetan Plateau and their impacts on energy and water cycle: a review, *Glob. Planet Change*,
775 112, 79-91, 2014.

776 Yao, T.D., Thompson, L., Yang, W., Yu, W.S., Gao, Y., Guo, X.J., Yang, X.X., Duan, K.Q., Zhao,
777 H.B., Xu, B.Q., Pu, J.C., Lu, A.X., Xiang, Y., Kattel, D.B., and Joswiak, D.: Different glacier
778 status with atmospheric circulations in Tibetan Plateau and surroundings, *Nat. Clim. Change*, 2,
779 1-5, 2012.

780 Yao, Y.J., Zhao, S.H., Zhang, Y.H., Jia, K., and Liu, M.: Spatial and decadal variations in potential
781 evapotranspiration of China based on reanalysis datasets during 1982-2010, *Atmosphere*, 5,
782 737-754, 2014.

783 Yin, G., Hu, Z.Y., Chen, X., and Tiyip, T.: Vegetation dynamics and its response to climate change
31 / 55

784 in Central Asia, *J. Arid Land*, 8, 375, 2016.

785 Yu, J., Zhang, G., Yao, T., Xie, H., Zhang, H., Ke, C., and Yao, R.: Developing daily cloud-free
786 snow composite products from MODIS Terra-Aqua and IMS for the Tibetan Plateau, *IEEE*
787 *Trans. Geosci. Remote Sens.*, 54(4), 2171-2180, 2015.

788 Yue, S., Pilon, P., Phinney, B., Cavadias, G.: The influence of autocorrelation on the ability to
789 detect trend in hydrological series, *Hydrol. Process.*, 16(9), 1807-1829, 2002.

790 Zhang, D., Liu, X., Zhang, Q., Liang, K., and Liu, C.: Investigation of factors affecting
791 inter-annual variability of evapotranspiration and streamflow under different climate conditions.
792 *J. Hydrol.*, doi:10.1016/j.jhydrol.2016.10.047, 2016.

793 Zhang, G., Xie, H., Yao, T., Liang, T., and Kang, S.: Snow cover dynamics of four lake basins
794 over Tibetan Plateau using time series MODIS data (2001-2100), *Water Resour. Res.*, 48(10),
795 W10529, 2012.

796 Zhang, K., Kimball, J.S., Nemani, R.R., and Running, S.W.: A continuous satellite-derived global
797 record of land surface evapotranspiration from 1983 to 2006, *Water Resour. Res.*, 46(9),
798 W09522, 2010.

799 Zhang, L., Su, F., Yang, D., Hao, Z., and Tong, K.: Discharge regime and simulation for the
800 upstream of major rivers over Tibetan Plateau, *J. Geophys. Res. Atmos.*, 118(15), 8500-8518,
801 2013.

802 Zhang, Q., Li, J., Singh, V., and Xu, C.: Copula-based spatial-temporal patterns of precipitation
803 extremes in China, *Int. J. Climatol.*, 33, 1140-1152, 2013.

804 Zhang, X., Tang, Q., Pan, M., and Tang, Y.: A long-term land surface hydrologic fluxes and states
805 dataset for China, *J. Hydrometeorol.*, 15, 2067-2084, 2014.

806 Zhang, Y., Peñá-Arancibia, J.L., McVicar, T.R., Chiew, F.H.S., Vaze, J., Liu, C.M., Lu, X.J.,
807 Zheng, H.X., Wang, Y.P., Liu, Y.Y., Miralles, D.G., and Pan, M.: Multi-decadal trends in global
808 terrestrial evapotranspiration and its components, *Scientific Reports*, 6, 19124, 2016.

809 Zhang, Y., Liu, C., Tang, Y., and Yang, Y.: Trend in pan evaporation and reference and actual
810 evapotranspiration across the Tibetan Plateau, *J. Geophys. Res.*, 112, D12110, 2007.

811 Zhou, C., Jia, S., Yan, H., and Yang, G.: Changing trend of water resources in Qinghai Province
812 from 1956 to 2000, *J. Glaciol. Geocryol.*, 27(3), 432-437, 2005 (in Chinese).

813 Zhou, J., Wang, L., Zhang, Y.S., Guo, Y.H., Li, X.P., and Liu, W.B.: Exploring the water storage
32 / 55

814 changes in the largest lake (Selin Co) over the Tibetan Plateau during 2003-2012 from a
815 basin-wide hydrological modeling,. *Water Resour. Res.*, 51, 8060-8086, 2015.

816 Zhou, S.Q., Kang, S., Chen, F., and Joswiak, D.R.: Water balance observations reveal significant
817 subsurface water seepage from Lake Nam Co., south-central Tibetan Plateau,. *J. Hydrol.*, 491,
818 89-99, 2013.

819 Zhou, S.Q., Wang, Z., and Joswiak, D.R.:From precipitation to runoff: stable isotopic fractionation
820 effect of glacier melting on a catchment scale, *Hydrol. Process.*, 28(8), 3341-3349, 2014.

821 Zhu, Y., Chen, J., Chen, G.: Runoff variation and its impacting factors in the headwaters of the
822 Yangtze River in recent 32 years, *J. Yangtze River Sci. Res. Inst.*, 28(6), 1-4, 2011 (in Chinese).

823 **Table 1:** Overview of multi-source datasets applied in this study

Data category	Data source	Spatial resolution	Temporal resolution	Available period used	Reference
Runoff (Q)	Observed, National Hydrology Almanac of China	—	Daily	1982-2011	—
	VIC_IGSNRR simulated	0.25°	Daily	1982-2011	Zhang et al. (2014)
Precipitation (P)	Observed, CMA	0.5°	Monthly	1982-2011	—
	TRMM 3B43 V7	0.25°	Monthly	2000-2011	Huffman et al. (2012)
	IGSNRR forcing	0.25°	Daily	1982-2011	Zhang et al. (2014)
Temperature (Temp.)	Observed, CMA	0.5°	Monthly	2000-2011	—
Terrestrial storage change (ΔS)	GRACE-CSR	Approx.300-400 km	Monthly	2002-2011	Tapley et al. (2004)
	GRACE-GFZ	Approx.300-400 km	Monthly	2002-2011	Tapley et al. (2004)
	GRACE-JPL	Approx.300-400 km	Monthly	2002-2011	Tapley et al. (2004)
Potential evaporation (PET)	CRU	0.5°	Monthly	1982-2011	Harris et al. (2013)
Actual evaporation (ET)	MTE_E	0.5°	Monthly	1982-2011	Jung et al. (2010)
	VIC_E	0.25°	Daily	1982-2011	Zhang et al. (2014)
	GLEAM_E	0.25°	Daily	1982-2011	Miralles et al. (2011)
	PML_E	0.5°	Monthly	1982-2011	Zhang Y et al. (2016)
	Zhang_E	8 km	Monthly	1983-2006	Zhang et al. (2010)
	GNoah_E	1.0°	3 hourly	1982-2011	Rui (2011)
NDVI	GIMMS NDVI dataset	8 km	15 daily	1982-2011	Tucker et al. (2005)
LAI	GLASS LAI Product	0.05°	8 daily	1982-2011	Liang and Xiao (2012)
Snow Cover	TP Snow composite Products	500 m	Daily	2005-2013	Zhang et al. (2012)
SWE	VIC_IGSNRR simulated	0.25°	Daily	1982-2011	Zhang et al. (2014)
	GlobSnow-2 Product	25 km	Daily	1982-2011	Takala et al. (2011)
Glacier Area	the Second Glacier Inventory Dataset of China	—	—	2005	Guo et al. (2014)

824 **Table 2:** Main features of the 18 TP river basins used in this study. The precipitation and temperature statistics for each basin were calculated from the observed
825 CMA datasets while the NDVI and LAI statistics were extracted from the GIMMS NDVI dataset and GLASS LAI product. The GA% and SC% represented the
826 percentages of multiyear-mean glacier cover and snow cover in each basin which were calculated from the Second Glacier Inventory Dataset of China and the daily
827 TP snow cover dataset (2005-2013)

828

No.	Station	Altitude (m)	River name	Drainage area (km ²)	Multiyear-mean (1982-2011) and basin-averaged parameters						
					Q (mm/yr)	Prec. (mm/yr)	Temp.(°C/yr)	NDVI	LAI	GA%	SC%
01	Kulukelangan	2000	Yerqiang	32880.00	158.60	128.34	-5.68	0.05	0.03	10.97	35.03
02	Tongguziluke	1650	Yulongkashi	14575.00	151.56	134.04	-4.07	0.06	0.04	23.27	35.95
03	Numaitilangan	1880	Keliya	7358.00	103.18	137.14	-4.78	0.06	0.03	10.86	29.16
04	Zelingou	4282	Bayin	5544.00	41.42	340.68	-4.98	0.13	0.09	0.09	21.22
05	Gadatan	3823	Yellow	7893.00	200.95	566.01	-4.60	0.34	0.54	0.13	14.94
06	Xining	3225	Yellow	9022.00	99.90	503.74	0.97	0.36	0.70	0.00	10.06
07	Tongren	3697	Yellow	2832.00	149.36	533.25	-1.37	0.39	0.83	0.00	9.42
08	Tainaihai	2632	Yellow	121972.00	159.48	540.32	-2.40	0.34	0.72	0.09	15.89
09	Huangheyan	4491	Yellow	20930.00	31.18	386.42	-4.81	0.23	0.61	0.00	17.25
10	Jimai	4450	Yellow	45015.00	85.50	441.48	-4.16	0.26	0.52	0.00	20.05
11	Yajiang	2599	Yalong	67514.00	237.66	717.05	-0.23	0.43	0.80	0.15	18.36
12	Zhimenda	3540	Yangtze	137704.00	96.23	405.66	-4.83	0.20	0.26	0.96	17.87
13	Jiaoyuqiao	3000	Salween	72844.00	364.26	620.88	-1.89	0.29	0.44	2.02	23.73
14	Pangduo	5015	Brahmaputra	16459.00	348.31	544.59	-1.53	0.27	0.33	1.66	23.33
15	Tangjia	4982	Brahmaputra	20143.00	350.61	555.17	-1.89	0.27	0.34	1.39	21.83
16	Gongbujiangda	4927	Brahmaputra	6417.00	586.96	692.06	-4.24	0.27	0.36	4.12	25.99
17	Nuxia	2910	Brahmaputra	191235.00	307.38	401.35	-0.73	0.22	0.25	1.90	13.50
18	Yangcun	3600	Brahmaputra	152701.00	163.25	349.91	-0.87	0.19	0.18	1.28	10.52

829

830 **Table 3:** Contribution of glacier-melt to discharge in 18 TP basins (“—” shows no glacier influences, “—*” shows the percentage is empirically estimated through
831 the relation between lacier area ratio and glacier melt for basins in which the glacier melt contribution has been reported in the literatures)
832

Basin	Contributions of glacier-melt to discharge (%)	Reference
Kulukelangan	62.7	Mansur and Ajnisa (2005)
Tongguziluoke	64.9	Liu J et al. (2016)
Numaitilangan	71.0	Chen (1988)
Zelingou	—	—
Gadatan	—	—
Xining	—	—
Tongren	—	—
Tainaihai	0.8	Zhang et al. (2013)
Huangheyuan	—	—
Jimai	—	—
Yajiang	1.4	—*
Zhimenda	6.5	Zhang et al. (2013)
Jiaoyuqiao	4.8	Zhang et al. (2013)
Nuxia	11.6	Zhang et al. (2013)
Pangduo	10.1	—*
Tangjia	8.5	—*
Gongbujiangda	25.2	—*
Yangcun	7.8	—*

833
834
835

836 **Table 4:** Annual-averaged water storage changes (ΔS) in 18 TP basins derived from GRACE retrievals (2002-2013) from three different processing centers (CSR,
837 GFZ and JPL)

838

Basin	Water storage Change (ΔS ,mm)		
	CSR	GFZ	JPL
Kulukelangan	-0.16	-0.16	-0.00
Tongguziluoke	0.10	0.10	0.28
Numaitilangan	0.24	0.22	0.41
Zelingou	0.63	0.41	0.69
Gadatan	0.02	-0.24	-0.03
Xining	-0.08	-0.35	-0.14
Tongren	-0.13	-0.41	-0.21
Tainaihai	0.12	-0.16	0.10
Huangheyan	0.60	0.35	0.70
Jimai	0.41	0.15	0.48
Yajiang	-0.23	-0.50	-0.21
Zhimenda	0.57	0.38	0.78
Jiaoyuqiao	-1.00	-1.13	-0.79
Nuxia	-1.42	-1.44	-1.31
Pangduo	-1.21	-1.29	-1.02
Tangjia	-1.40	-1.46	-1.24
Gongbujiangda	-1.61	-1.67	-1.47
Yangcun	-1.33	-1.34	-1.21

839

840

841 **Table 5:** Nonparametric trends for different ET estimates during the period 1982-2006 detected by modified Mann-Kendall test, the bold number showed the
 842 detected trend is statistically significant at the 0.05 level

843	Basin	ET _{wb}	GLEAM_E	VIC_E	Zhang_E	PML_E	MET_E	GNoah_E
844								
845	Kulukelangan	-0.09	0.09	0.18	–	0.03	-0.01	0.07
	Tongguziluoke	-0.02	0.10	0.13	–	0.03	-0.08	0.19
846	Numaitilangan	0.04	0.10	0.14	–	0.14	-0.10	0.22
	Zelingou	0.13	0.23	0.11	0.09	0.04	0.06	0.02
847	Gadatan	-0.09	0.25	0.070	-0.10	-0.01	0.06	-0.07
	Xining	-0.06	0.54	0.01	-0.08	0.01	0.02	-0.06
848	Tongren	-0.06	0.34	-0.15	-0.17	0.07	0.02	0.13
	Tainaihai	0.06	0.28	-0.03	-0.11	0.04	0.05	0.04
849	Huangheyang	0.08	0.19	-0.01	-0.10	0.08	0.05	0.10
	Jimai	-0.07	0.23	-0.01	-0.08	0.03	0.05	0.10
850	Yajiang	0.17	0.26	0.06	-0.21	-0.01	0.03	-0.02
	Zhimenda	0.11	0.28	0.10	0.01	0.07	0.04	0.07
851	Jiaoyuqiao	0.18	0.28	0.10	-0.11	0.05	0.05	0.07
	Nuxia	-0.09	0.25	0.09	-0.10	0.12	0.04	0.10
852	Pangduo	0.05	0.28	0.17	-0.07	0.07	0.07	0.11
	Tangjia	0.09	0.26	0.17	-0.09	0.20	0.06	0.12
853	Gongbujiangda	-0.26	0.12	0.13	-0.16	0.19	0.01	0.15
	Yangcun	0.03	0.28	0.08	-0.06	0.10	0.04	0.09

854

855

856 **Figure captions:**

857 **Figure1.** Map of river basins and hydrological gauging stations (green dots) over the
858 Tibetan Plateau (TP) used in this study. The grey shading shows the topography of TP
859 in meters above the sea level and the blue shading exhibits the glaciers distribution in
860 TP extracted from the Second Glacier Inventory Dataset of China.

861 **Figure 2.** Comparison of VIC_IGSNRR simulated and observed monthly runoff for
862 Tangnaihai and Panduo stations (a and b) as well as (c) basin-averaged monthly
863 TRMM, CMA gridded and IGSNRR forcing precipitations for the smallest basin
864 (Tongren station) over the period 1982-2011. (d) shows the comparison of TRMM
865 (blue) and IGSNRR forcing (red) precipitations against CMA gridded precipitation for
866 18 river basins over TP during the period 2000-2011.

867 **Figure 3.** Comparison of different ET products against the calculated ET through the
868 water balance method (ET_{wb}) at the monthly time scale for 18 TP basins during the
869 period 1983-2006. The boxplot of monthly estimates of different ET products for 18
870 TP basins are shown in (a) while the correlation coefficients and
871 root-mean-square-errors (RMSEs, mm/month) for each ET product relatively to ET_{wb}
872 are exhibited in (b).

873 **Figure 4.** General water and energy status (a. the perspective of Budyko framework)
874 and their relationships with glacier (b) and vegetation (c and d) for eighteen TP river
875 basins (1983-2006). The ET used in this figure is calculated from the bias-corrected
876 water balance method.

877 **Figure 5.** Seasonal cycles (1982-2011) of water budget components in westerlies-
878 dominated (column 1), East Asian monsoon-dominated (columns 2-4) and Indian
879 monsoon-dominated (columns 5-6) TP basins.

880 **Figure 6.** Seasonal cycles (1982-2011) of air temperature and vegetation parameters
881 in westerlies-dominated (column 1), East Asian monsoon-dominated (columns 2-4)
882 and Indian monsoon-dominated (columns 5-6) TP basins.

883 **Figure 7.** Seasonal cycles (1982-2011) of snow cover and snow water equivalent
884 (SWE) in westerlies-dominated (column 1), East Asian monsoon-dominated (columns

885 2-4) and Indian monsoon-dominated (columns 5-6) TP basins. The snow cover was
886 extracted from cloud free snow composite product during the period 2005-2013. It
887 should also be noted that the GlobSnow data are not available for some basins.

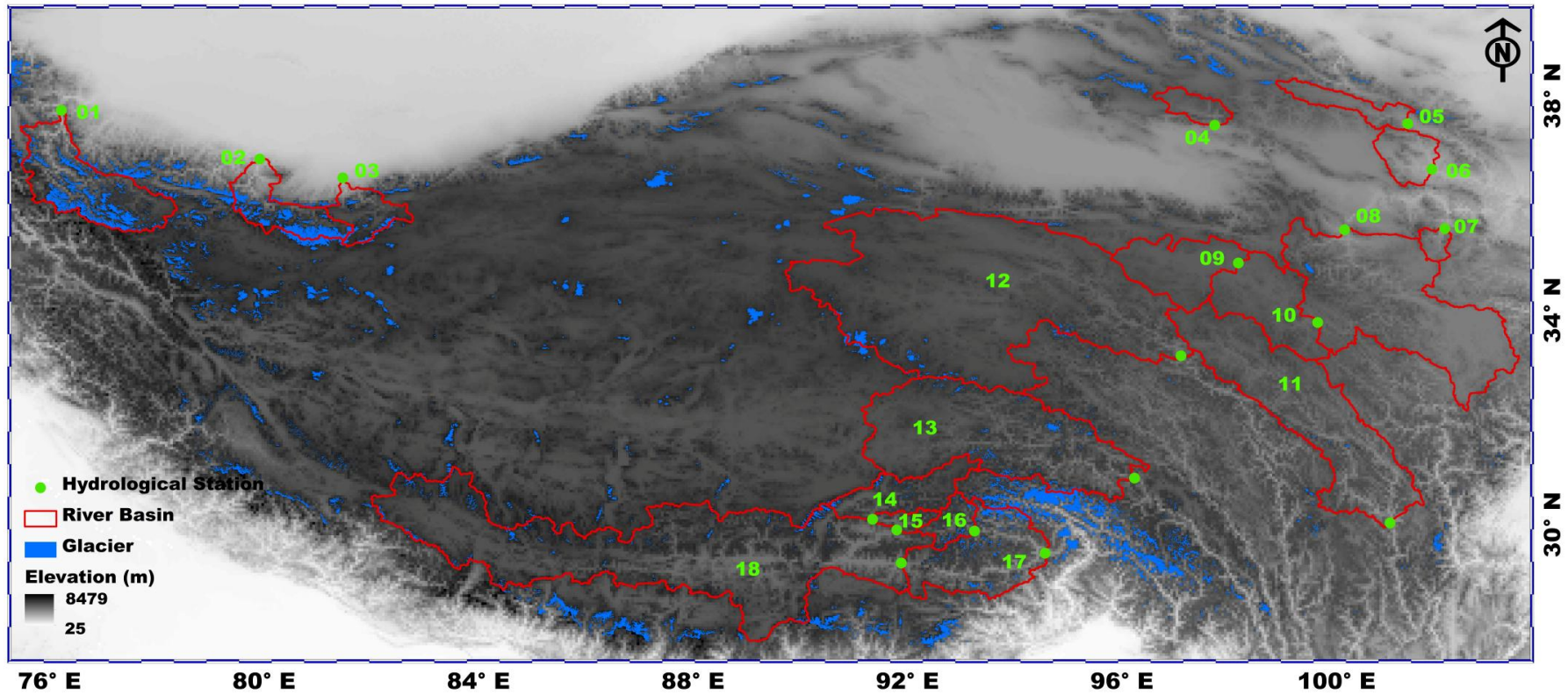
888 **Figure 8.** Sen's slopes of water budget components and vegetation parameters in
889 westerlies-dominated TP basins during the period of 1982-2011. The double red stars
890 showed that the trend was statistically significant at the 0.05 level.

891 **Figure 9.** Linear and non-parametric trends of westerly, Indian monsoon and East
892 Asian summer monsoon during the period 1982-2011 revealed prospectively by the
893 Asian Zonal Circulation Index, Indian Ocean Dipole Mode Index and East Asian
894 Summer Monsoon Index.

895 **Figure 10.** Similar to Figure 8 but for East Asian monsoon-dominated TP basins. It
896 should be noted that the GlobSnow data are not available for some basins. The double
897 red stars showed that the trend was statistically significant at the 0.05 level.

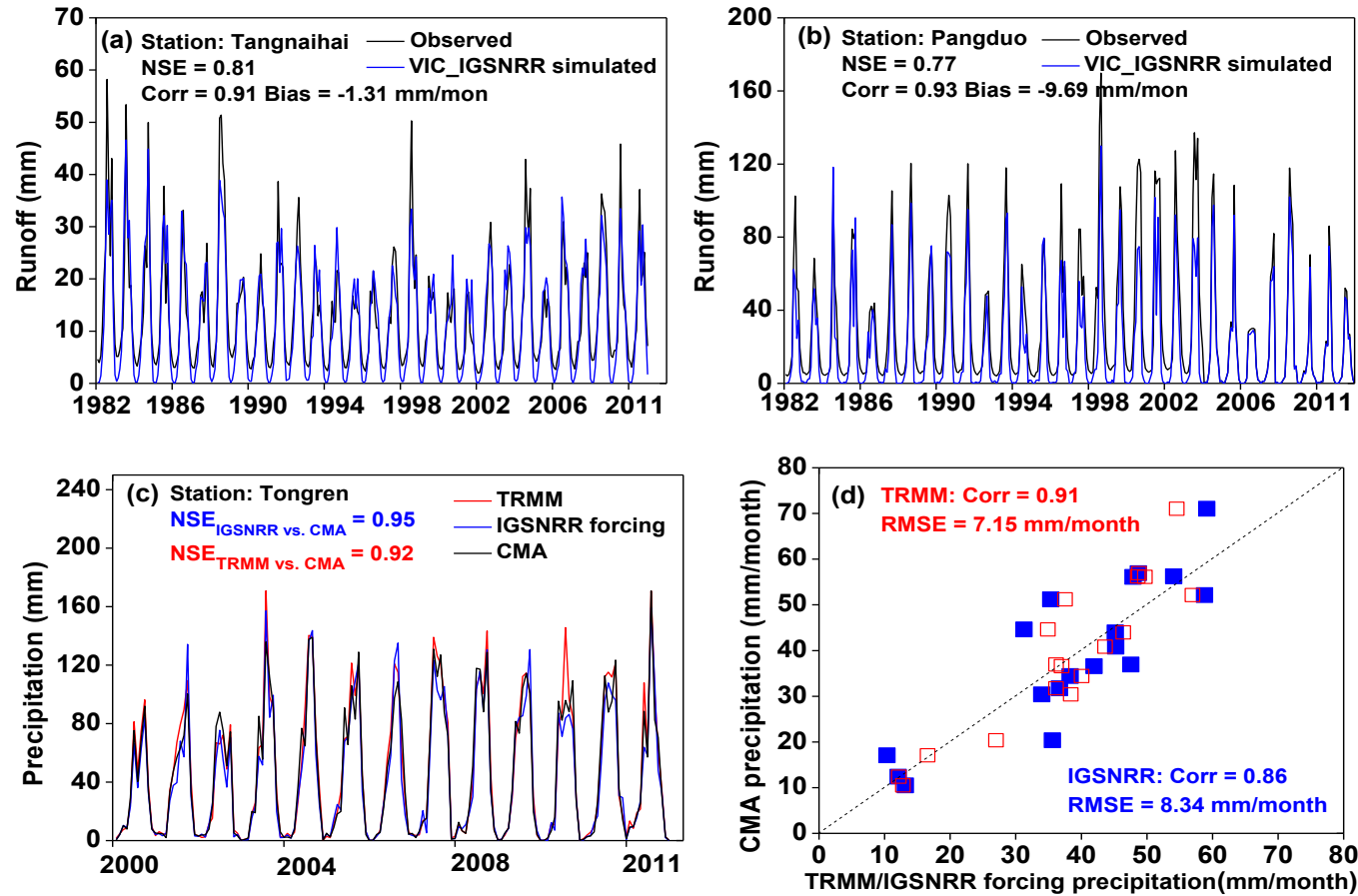
898 **Figure 11.** Similar to Figure 8 but for Indian monsoon-dominated TP basins. It should
899 be noted that the GlobSnow data are not available for some basins. The double red
900 stars showed that the trend was statistically significant at the 0.05 level.

901 **Figure 1.** Map of river basins and hydrological gauging stations (green dots) over the Tibetan Plateau (TP) used in this study. The grey shading shows the
902 topography of TP in meters above the sea level and the blue shading exhibits the glaciers distribution in TP extracted from the Second Glacier Inventory Dataset of
903 China.



904
905

906 **Figure 2.** Comparison of VIC_IGSNRR simulated and observed monthly runoff for Tangnaihai and Panduo stations (a and b) as well as (c) basin-averaged
 907 monthly TRMM, CMA gridded and IGSNRR forcing precipitations for the smallest basin (Tongren station) over the period 1982-2011. (d) shows the comparison of
 908 TRMM (blue) and IGSNRR forcing (red) precipitations against CMA gridded precipitation for 18 river basins over TP during the period 2000-2011.

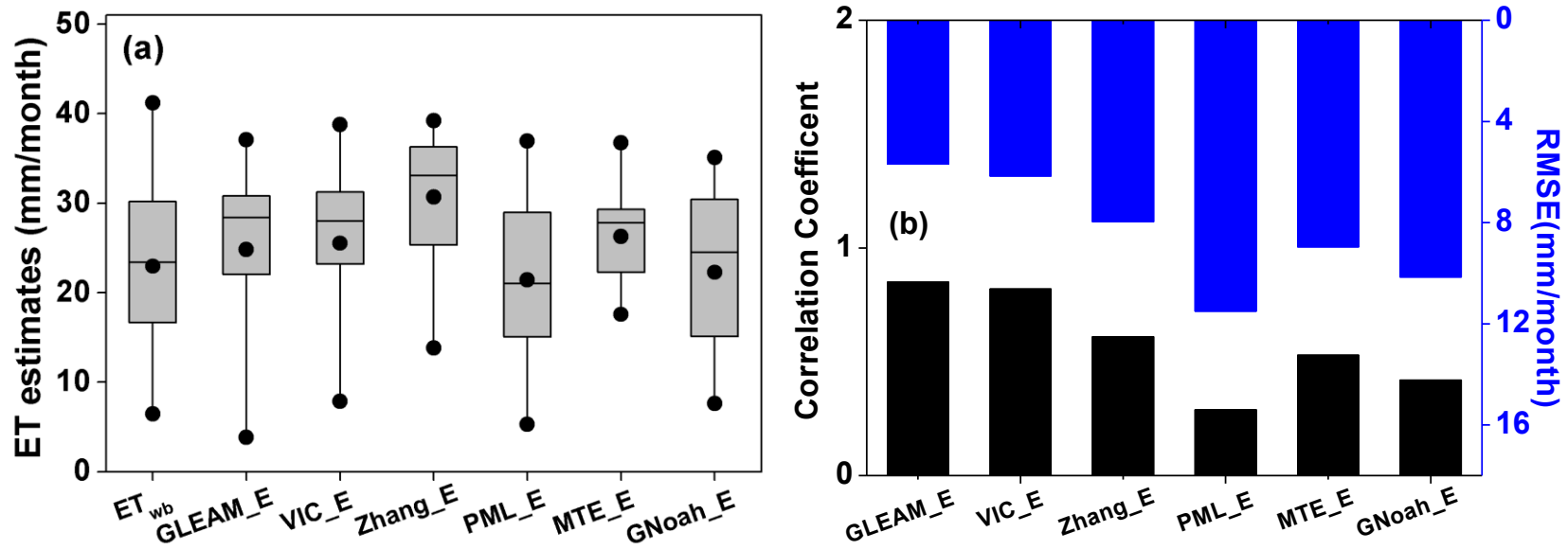


909

910

911

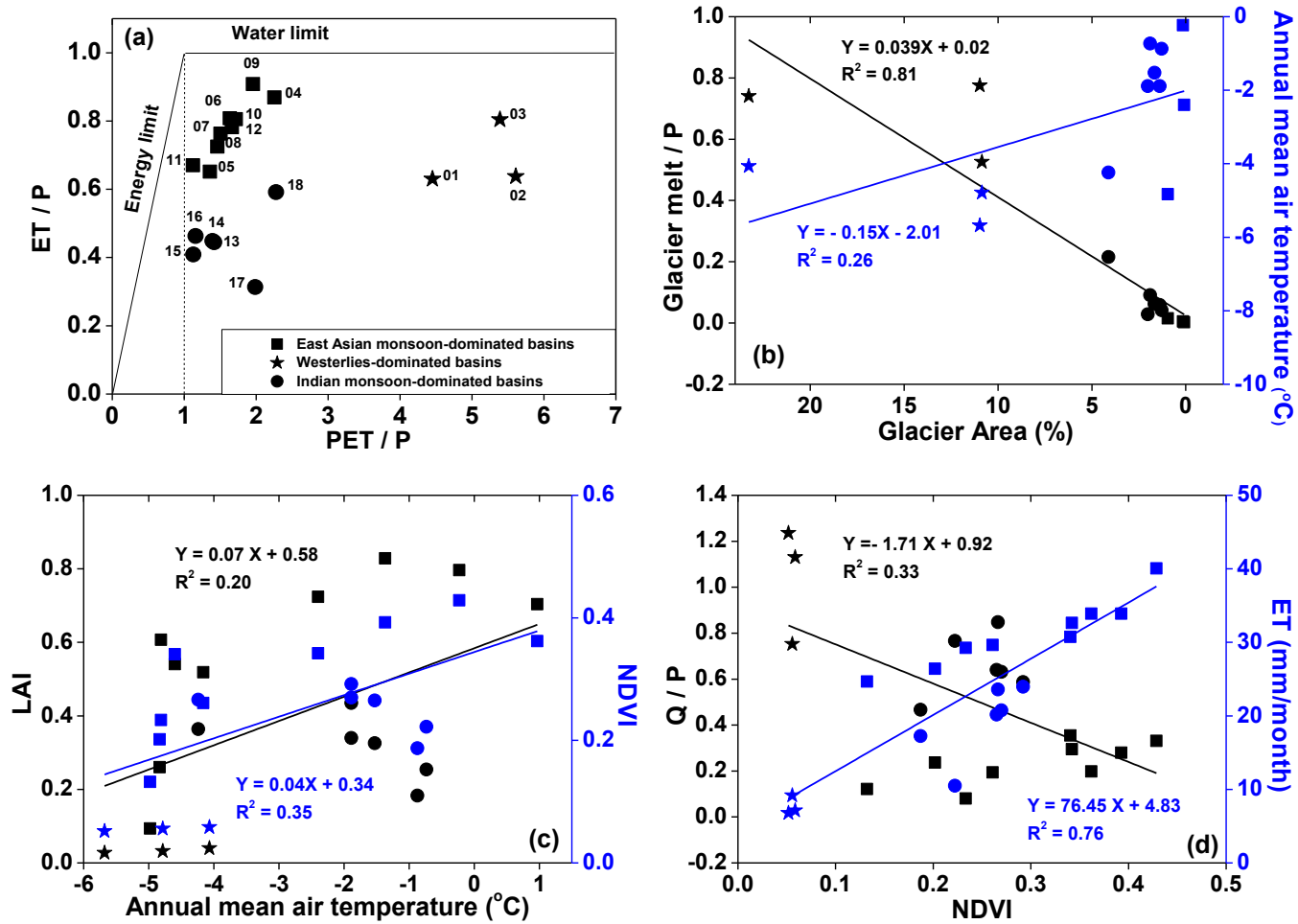
912 **Figure 3.** Comparison of different ET products against the calculated ET through the water balance (ET_{wb}) at the monthly time scale for 18 river basins over the
 913 Tibetan Plateau during the period 1983-2006. The boxplot of monthly estimates of different ET products for 18 TP basins are shown in (a) while the correlation
 914 coefficients and root-mean-square-errors (RMSEs, mm/month) for each ET product relatively to ET_{wb} are exhibited in (b).



915

916

917 **Figure 4.** General water and energy status (a. the perspective of Budyko framework) and their relationships with glacier (b) and vegetation (c and d) for eighteen
 918 TP river basins (1983-2006). The ET used in this figure is calculated from the bias-corrected water balance method.

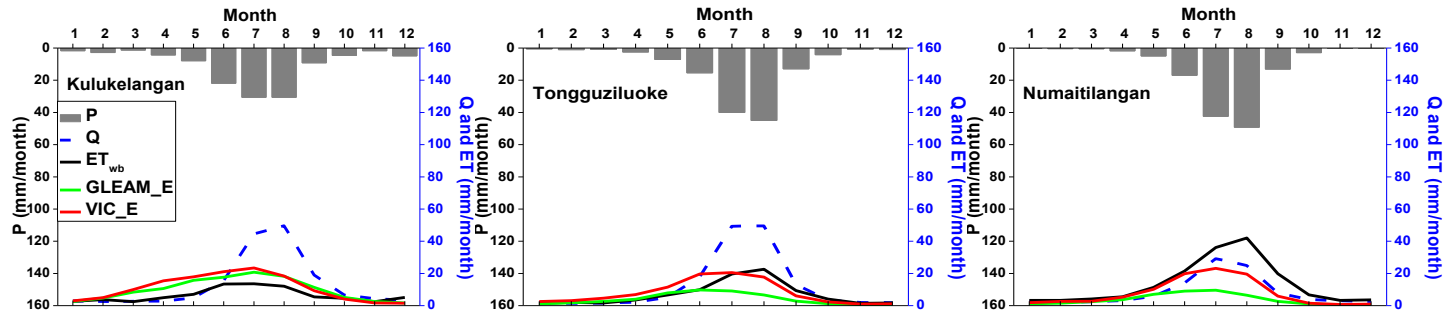


919

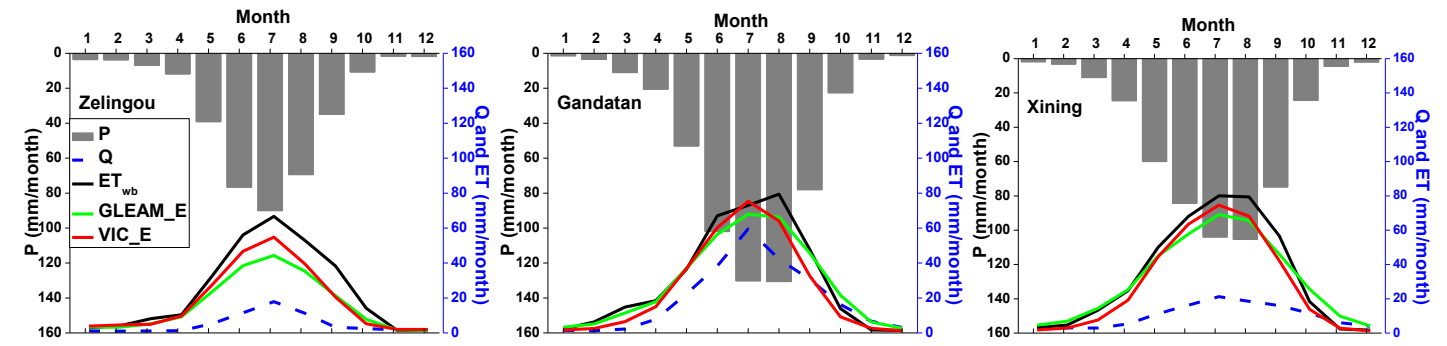
920

921 **Figure 5.** Seasonal cycles (1982-2011) of water budget components in westerlies-dominated (column 1), East Asian monsoon-dominated (columns 2-4) and Indian
 922 monsoon-dominated (columns 5-6) TP basins.

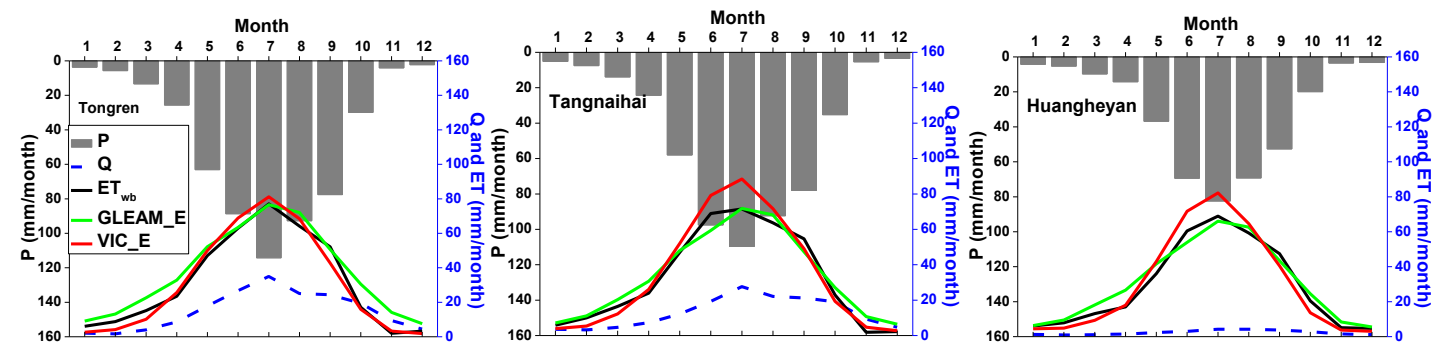
923



924



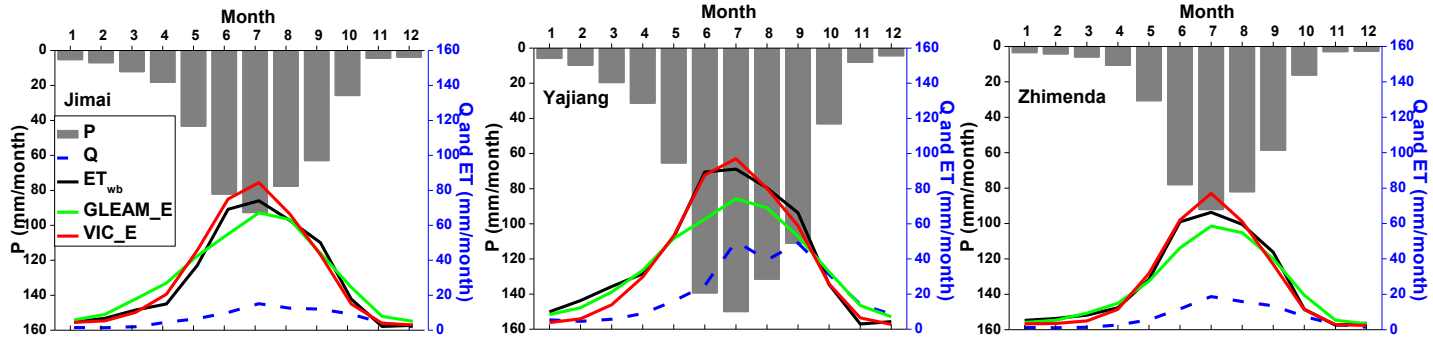
925



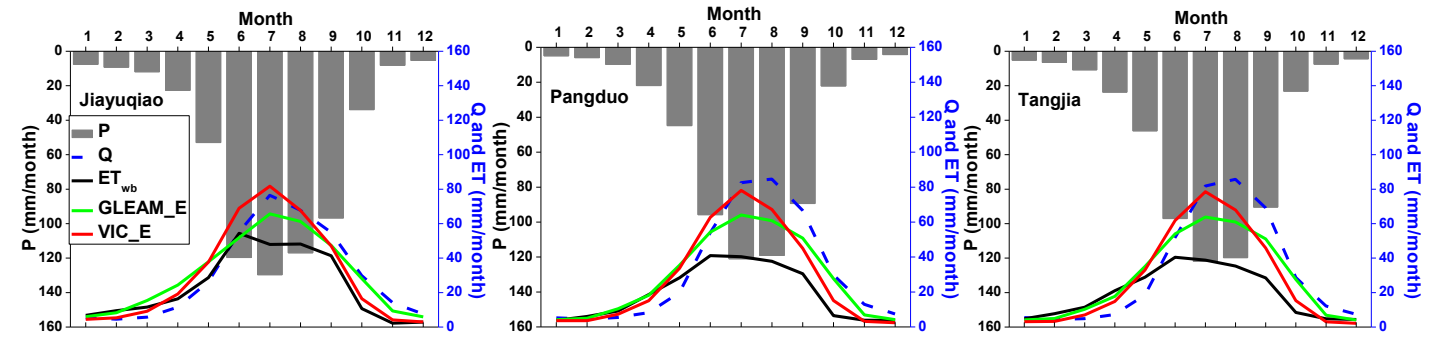
926

Figure 5: (continued)

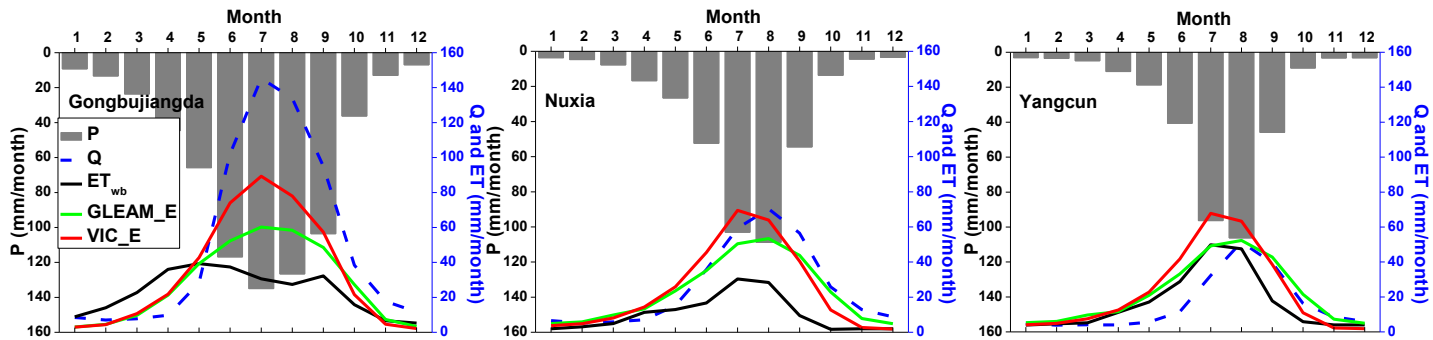
927



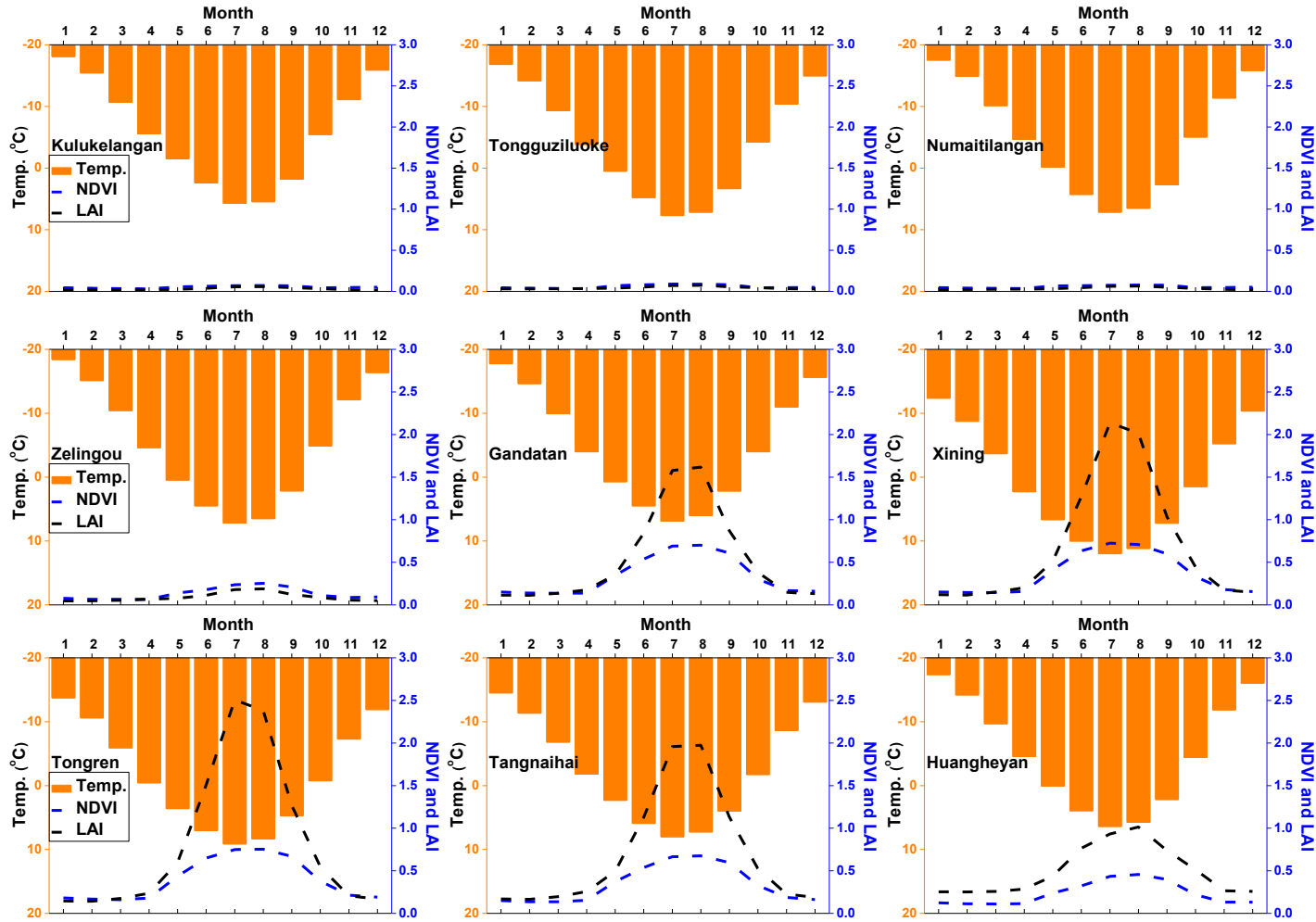
928



929



930 **Figure 6.** Seasonal cycles (1982-2011) of air temperature and vegetation parameters in westerlies-dominated (column 1), East Asian monsoon-dominated (columns
 931 2-4) and Indian monsoon-dominated (columns 5-6) TP basins.



932

933

934

935

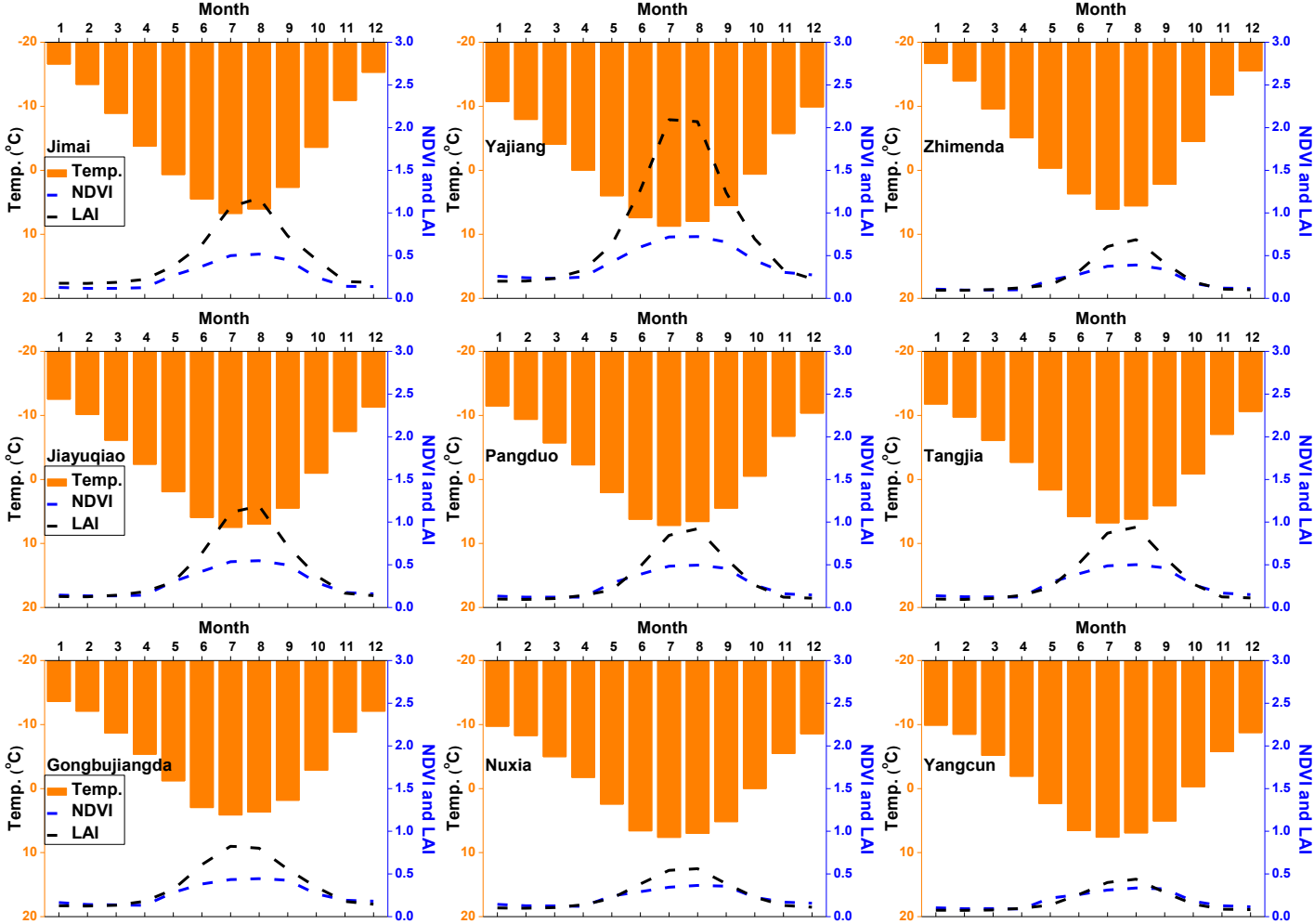
936

937

938

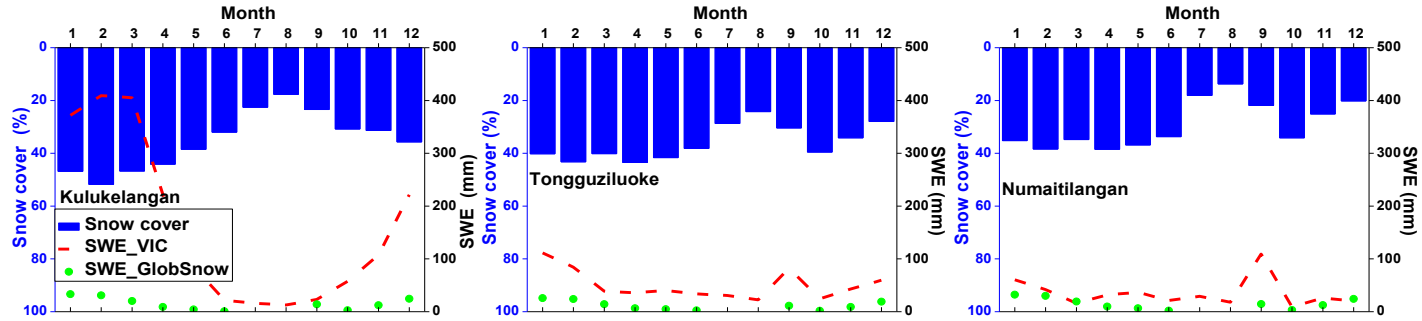
939

Figure 6: (continued)

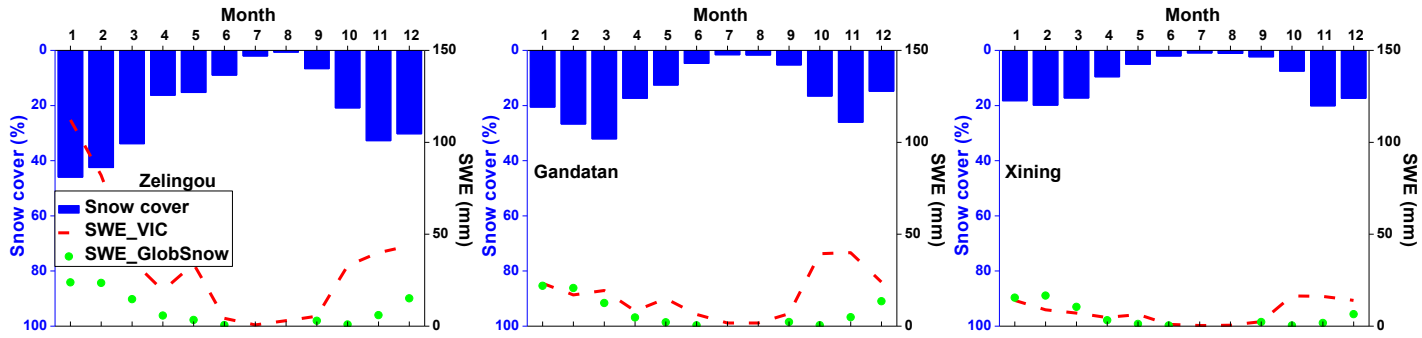


940 **Figure 7.** Seasonal cycles (1982-2011) of snow cover and snow water equivalent (SWE) in westerlies-dominated (column 1), East Asian monsoon- dominated
941 (columns 2-4) and Indian monsoon-dominated (columns 5-6) TP basins. The snow cover was extracted from cloud free snow composite product during the period
942 2005-2013. It should also be noted that the GlobSnow data are not available for some basins.
943

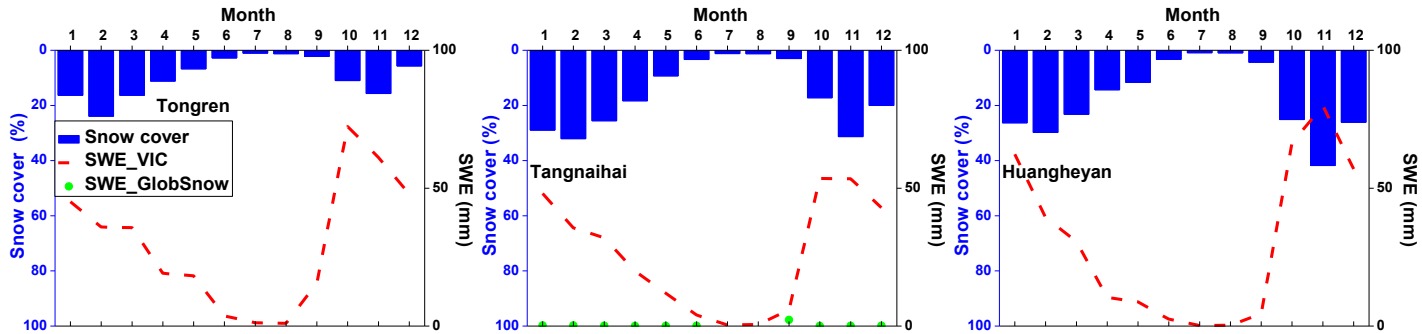
944



945



946

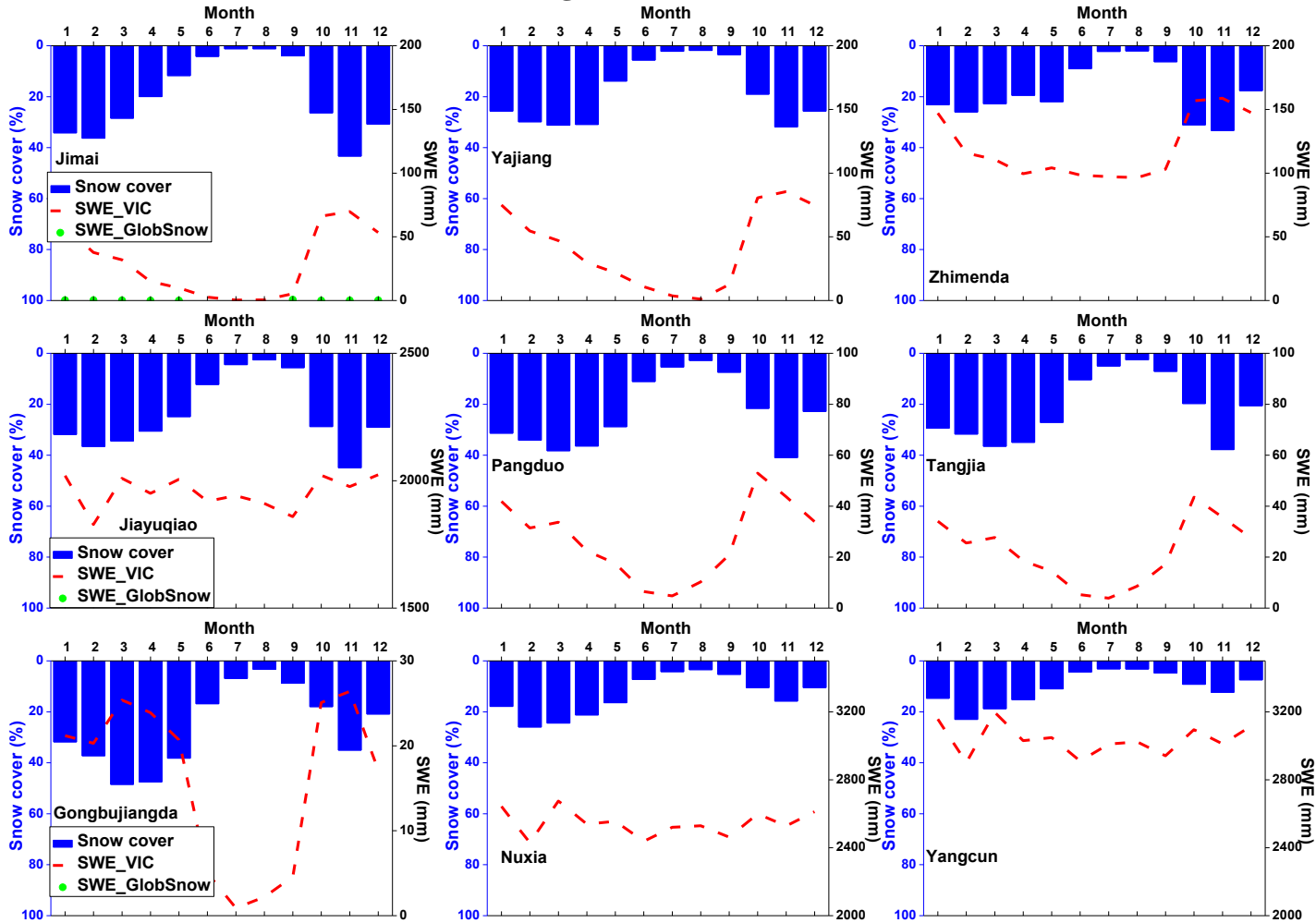


947

948

949

Figure 7: (continued)



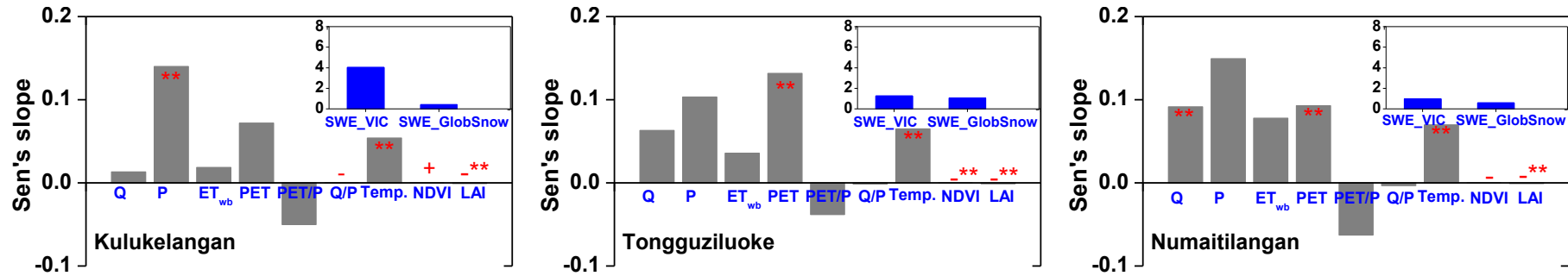
950

951

952

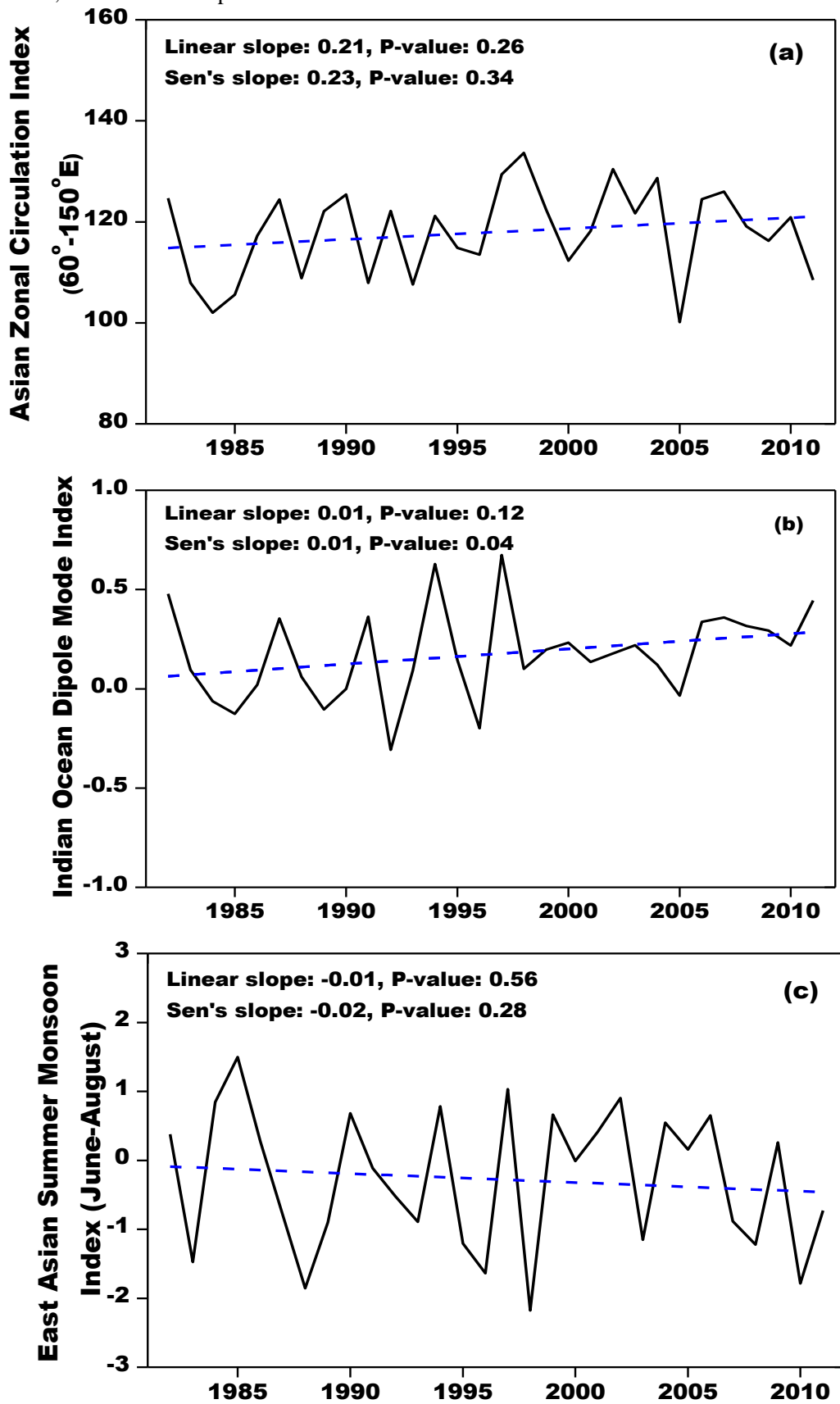
953

954 **Figure 8.** Sen's slopes of water budget components and vegetation parameters in westerlies-dominated TP basins during the period of 1982-2011. The double red
 955 stars showed that the trend was statistically significant at the 0.05 level.



956
 957

958 **Figure 9.** Linear and non-parametric trends of westerly, Indian monsoon and East Asian summer
 959 monsoon during the period 1982-2011 revealed prospectively by the Asian Zonal Circulation
 960 Index, Indian Ocean Dipole Mode Index and East Asian Summer Monsoon Index.

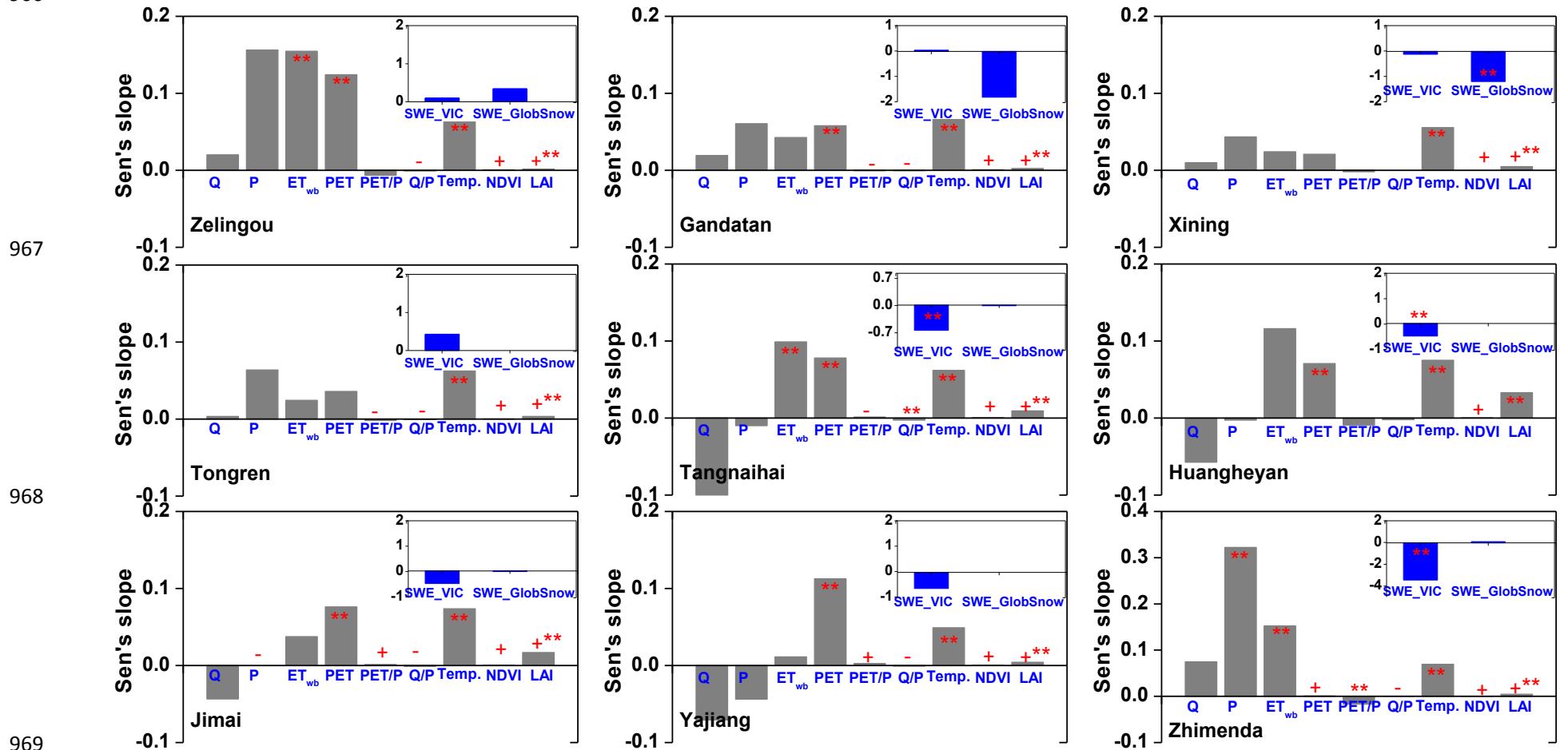


961

962

963

964 **Figure 10.** Similar to Figure 8 but for East Asian monsoon-dominated TP basins. It should be noted that the GlobSnow data are not available for some basins. The
 965 double red stars showed that the trend was statistically significant at the 0.05 level.
 966



972 **Figure 11.** Similar to Figure 8 but for Indian monsoon-dominated TP basins. It should be noted that the GlobSnow data are not available for some basins. The
 973 double red stars showed that the trend was statistically significant at the 0.05 level.
 974

